BOEING

PG-3
International Space Station Program

D683-56171-1

Integrated ISPR Structural Analysis for Fluid Combustion Facility Combustion Integrated Rack - Preliminary Design

Revision New

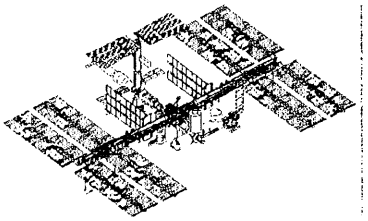

INTERNATIONAL SPACE STATION

December 14, 1998

Submitted to: The Boeing Company
Houston, Texas
Contract Number NAS15-10000 (DR FP02)

INTEGRATED ISPR STRUCTURAL ANALYSIS FOR FLUID COMBUSTION FACILITY COMBUSTION INTEGRATED RACK - PRELIMINARY DESIGN

(D683–56171-1)
REV NEW
DECEMBER 14, 1998

Boeing Defense & Space Group
Missiles & Space Division
(a division of The Boeing Company)
Huntsville, Alabama

PREPARED BY:	C. Welch C.T. Welch	2-8263	12-14-98
PREPARED BY:	S. Kerkhof S.L. Kerkhof	2-8263	12/14/98
CHECKED BY:	J. Heflin J Heflin	2-8263	12/14/98
APPROVED BY:	T. Helsper T. Helsper	2-8263	12/16/98
DQA:	R. Hudson Ricci Hudson	2-8641	98-12-18

(This Page Intentionally Blank)

ABSTRACT

This report contains the preliminary design structural analysis of the ISPR for the Fluid Combustion Facility (FCF) Combustion Integrated Rack (CIR). This report includes requirements summary, analytical methods used, analysis results, and conclusions and recommendations. This preliminary design structural analysis is submitted in accordance with documentation requirement FP02 of ECP 438 to NAS15-10000 to verify that the integrated rack meets the structural requirements as defined in SSP 52005B.

KEYWORDS

Structural Analysis

Internal Space Station

Fluid Combustion Facility

Combustion Integrated Rack

ISPR

Fracture Analysis

FCF

CIR

Preliminary Design Analysis

(This Page Intentionally Blank)

DOC NO. D683-56171-1

DOCUMENT RELEASE RECORD (DRR)

RELEASES (& DATES)	Update this document by: ACTIVE PAGES	PAGES ADDED	PAGES DELETED	AUTHORIZATIONS (& REMARKS)
Rev New 12/14/98	i-xii 1-1 thru 1-6 2-1 thru 2-4 3-1 thru 3-10 4-1 thru 4-4 5-1 thru 5-4 6-1 thru 6-16 7-1 thru 7-6 8-1 thru 8-18			NAS15-10000 (DR FP02)

Erin Lina Campbell 1-22-99

DOC NO. D683-56171-1

DOCUMENT RELEASE RECORD (DRR)

RELEASES (& DATES)	Update this document by:			AUTHORIZATIONS (& REMARKS)
	ACTIVE PAGES	PAGES ADDED	PAGES DELETED	

TABLE OF CONTENTS

TABLE OF CONTENTS (CONTINUED)

LIST OF TABLES

TABLE OF CONTENTS (CONTINUED)

LIST OF TABLES

LIST OF FIGURES

TABLE OF CONTENTS (CONTINUED)

LIST OF FIGURES

ABBREVIATIONS AND ACRONYMS

APM	Attached Pressurized Module
ARIS	Active Rack Isolation System
C	Celsius
CAM	Centrifuge Accommodation Module
CFM	Cubic Feet per Minute
CIR	Combustion Integrated Rack
dB	Decibel
DOF	Degree of Freedom
DQA	Drawing Quality Assurance
DRR	Document Release Record
F	Fahrenheit
FCA/PCA	Functional Configuration Audit/Physical Configuration Audit
FCF	Fluid Combustion Facility
FEM	Finite Element Model
FEMAP	Finite Element Modeling and Postprocessing Software
FLG	Flange
FS	Factor of Safety
FT	Foot, Feet
FTG	Fitting
g	Gravitational constant
Grms	G-Root Mean Square
Hg	Mercury
Hz	Hertz
ICD	Interface Control Document
ID	Identification
IN-LB	Inch-pounds
INCAP	Interactive Composite Analysis Program
ISPR	International Standard Payload Rack
ISS	International Space Station

JEM	Japanese Experiment Module
K	Kilo
KSI	Thousand pounds per square inch
LBF	Pounds force
LBS	Pounds
M	Meter
M/S	Meters per second
MIN	Minimum
MM	Millimeter
MPC	Multipoint Constraint
MS	Margin of Safety
MPLM	Mini Pressurized Logistics Module
MSC/NASTRAN	MacNeal-Schwendler Finite Element Code
MSFC	Marshall Space Flight Center
N	Newtons
NASA	National Aeronautics and Space Administration
Pa	Pascals
PG-3	Boeing - Huntsville
psia	Pounds per Square Inch, Absolute
PSD	Power Spectral Density
QUAD	NASTRAN plate shell element
RAD	Radian
RSR	Resupply Stowage Rack
SEC	Seconds
SQRT	Square root
SSP	Space Station Program
STS	Space Transportation System
ULT	Ultimate
USL	United States Laboratory Module
VLAM	V-22, Laminate Analysis Code

SECTION 1

INTRODUCTION

1.1 GENERAL INFORMATION

This report presents the preliminary design analysis of the integrated ISPR for the Combustion Integrated Rack (CIR) of the Fluid Combustion Facility (FCF). The CIR is integrated into an ARIS equipped ISPR. The CIR is part of the FCF and is managed by NASA Lewis Research Center. It is scheduled to fly on an MPLM on Space Station Flight UF-3.

The preliminary design analysis is intended to be a quick look analysis of the integrated rack. This report documents the analysis of the ISPR and its interface to the payload and the module. The analysis of the payload will be performed by NASA Lewis Research Center personnel. Because this is a preliminary design analysis, it should be expected that some of the design details will change in the future. A second report is scheduled to analyze the final configuration.

The CIR consists of an ARIS equipped ISPR, an optical bench, a thermal conditioning unit, control electronics, and support structure. A finite element model of the payload integrated into an ISPR was provided by NASA Lewis. All of the information about the payload contained in this report is based on data contained in the finite element model and represents the configuration that is represented in the model.

The rack is analyzed for the MPLM load factors contained in SSP41017 "Rack to MPLM ICD". Every combination of load factors are not included in this report. Since the ISPR has already been analyzed for a verification payload, that analysis is used to select critical combinations of load factors. There is additional information on the selection of critical loads in the analysis sections.

Thermal loads typically account for a small percentage of the total load in the rack. The initial analysis does not include the effects of temperature however a thermal case was run to show that thermal loads are small for the CIR. This is documented in Section 8.3.

Fatigue and fracture analyses were not performed for this preliminary design analysis. The stresses for the CIR are less than the stresses in the ISPR verification analysis, therefore it is expected that the fatigue /fracture analysis will show greater life.

The payload is subjected to random vibration loads and component accelerations. These loads were applied to the optical bench to calculate interface loads at the post. This analysis is presented in Section 8.2. The control electronics and thermal conditioning unit random vibration loads are not included in this preliminary design report, because the payload interface is typically more critical.

A dynamic model was prepared to calculate normal modes and frequencies. The results are described in Section 7.0. The CIR meets the 25 hz frequency requirement for an integrated rack.

The MSC/NASTRAN (Version 70) finite element code was used for static and dynamic analysis. A combination of finite element results and/or classical analysis methods were used to demonstrate that structural requirements were met. The FEMAP pre/post-processor program was used for model preparation and graphical display of results.

1.2 SUMMARY OF RESULTS

For this Preliminary Design Analysis, two criteria are considered:

1. Rack Strength with the integrated payload under the prescribed operational loads, and

2. Rack Strength in local areas under component loads.

Analysis Results for primary components checked under criteria 1 are summarized in Table 1-I. Results for local area subjects to components loads criteria is summarized in Table 1-II.

TABLE 1-I MINIMUM MARGINS OF SAFETY SUMMARY INTEGRATED LOADS

PART NAME	FAILURE MODE	MS(Limit)	MS(Ult)	PAGE NO.
Attach FTG	X-Flange Bending	0.53	0.43	8.0-4
Attach FTG	Y-Flange Bending	0.52	0.42	8.0-4
Flg/Skin Joint	Fastr Bearing	-	0.02	8.0-8
Posts	Web Strain	-	0.50	8.0-10
Posts	Cap Strain	-	0.23	8.0-11
Noodle	Bending	1.85	2.91	8.0-12
Noodle	Pull Off	0.38	0.63	8.0-12
Fasteners	Post Bearing	-	0.57	8.0-14

TABLE 1-II MINIMUM MARGINS OF SAFETY SUMMARY COMPONENT LOADS

PART NAME	FAILURE MODE	MS(Limit)	MS(Ult)	PAGE NO.
Noodle	Bending	0.35	0.35	8.0-12
Noodle	Pull Off	-0.09	0.09	8.0-12
Fasteners	Post Bearing	-	-0.16	8.0-14

Thermal effects were investigated and are not a significant consideration. See Section 8.3.

1.2.1 Discussion of Results

The preliminary design analysis shows positive margins in most locations. There are negative margins of safety for the noodle and fastener bearing in the post. Both of these margins are calculated for component loads. The component loads used for this preliminary design analysis are a conservative worst on worst combination of x, y, and z loads. Also there are techniques available to reduce the effect of random vibration in the component loads. A more detailed analysis should result in positive margins of safety at these locations, but they should be monitored during final design to ensure positive margins.

1.2.2 Life Summary of Fracture Critical Parts

Fracture analysis was not performed for the CIR for the preliminary design analysis. No fracture issues are expected because the CIR is enveloped by the ISPR analysis. Life and fracture for the CIR will be addressed in the final report.

SECTION 2

APPLICABLE DOCUMENTS

2.1 Government Document

MIL-HDBK-5 Rev. F 1 November 1990	Metal Material and Element for Aerospace Vehicle Structures
MSFC-STD-486 Rev. B 23 November 1990	Standard Threaded Fasteners, Torque Limit for
NSTS-08307 October 1989	Criteria for Preloaded Bolts
NSTS-14046 Rev. C April 1994	Payload Verification Requirements - National Space Transportation System Program
SSP-30558 Rev. B 30 June 1994	Fracture Control Requirements for Space Station
SSP-30559 Rev. B 30 June 1994	Structural Design and Verification Requirements, International Space Station Alpha
SSP-41017	Rack to Mini Pressurized Logistics Module Interface Control Document (ICD)
SSP-52005	Payload Flight Equipment Requirements and Guidelines for Safety Critical Structure
SSP-57000	Pressurized Payloads Interface Requirements Document
SSP-57007	International Standard Payload Rack (ISPR) Structural Integrator's Handbook

2.2 Boeing Documents

901-930-022 9 December 1987	V-22 Material Substantiating Data and Analysis Report
D180-27901-1 24 March 1984	INCAP-Interactive Composite Analysis Program
D683-30037-3	ISPR 6-Post Configuration FCA/PCA Stress/Fracture/Fatigue Analysis Report, Draft 2
D683-30037-6	Resupply/Stowage Rack (RSR) FCA/PCA Stress/Fracture/Fatigue Analysis Report, Rev. New

(This Page intentionally Left Blank)

SECTION 3

DESIGN REQUIREMENTS

3.1 Summary of Requirements

Program wide documents:

SSP 52005	Payload Flight Equipment Requirements and Guidelines for Safety-Critical Structures
SSP 57000	Pressurized Payloads Interface Requirements Document
SSP41017	Rack to Mini Pressurized Logistics Module Interface Control Document

3.2 Environment

The following are a reduced set of design environments used in the ISPR Rack analysis. They are shown here for reference only. A complete set of requirements can be found in SSP 52005, Rev. B, Section 4.0.

- Thermal and Pressure Environments (Ref. SSP 57000, Rev. B, Table 3.9.3.4-1)

  The ISPR Rack shall meet the performance requirements specified herein after exposure to the following thermal and pressure environments.

  Additional load cases and local loading conditions due to pressure differentials are also found in SSP 41017, Part 1, Rev. C, Paragraph 3.2.1.4.4.

TABLE 3-I ENVIRONMENTAL CONDITIONS

Environmental Conditions	Value
Atmospheric Conditions	
Pressure Extremes	0 to 104.8 kPa (0 to 15.2 psia)
Dewpoint	4.4 to 15.6°C (40 to 60 °F)
Percent relative humidity	25 to 75
Carbon dioxide partial pressure during nominal operations with 6 crewmembers plus animals	24-hr average exposure 5.3 mm Hg Peak exposure 7.6 mm Hg
Carbon dioxide partial pressure during crew changeout with 11 crewmembers plus animals	24-hr average exposure 7.6 mm Hg Peak exposure 10 mm Hg
Cabin air temperature in USL, JEM, APM, and CAM	17 to 28 °C (63 to 82 °F)
Cabin air temperature in Node 1	17 to 31 °C (63 to 87 °F)
Air velocity	0.051 to 2.03 m/s (10 to 40 ft/min)
Airborne microbes	< 1000 CFU/m3
Atmosphere particulate level	Average less than 100,000 particles/ft3 for particles less than 0.5 microns in size
MPLM Air Temperature	**Active Flights**
Pre-Launch	14 to 30 °C (57.2 to 86 °F)
Launch/Ascent	20 to 30 °C (68 to 86 °F)
On-Orbit (Cargo Bay + Deployment)	16 to 46 °C (60.8 to 114.8 °F)
On-Orbit (On-Station)	16 to 43 °C (63 to 109.4 °F)
On-Orbit (Retrieval + Cargo Bay)	11 to 45 °C (63 to 113°F)
Descent/Landing	10 to 42 °C (50 to 107.6 °F)
Post-Landing	10 to 42 °C (50 to 107.6 °F)
Ferry Flight	15.5 to 30 °C (59.9 to 86 °F)
	Passive Flights
Pre-Launch	15 to 24 °C (59 to 75.2 °F)
Launch/Ascent	14 to 24 °C (57.2 to 75.2 °F)
On-Orbit (Cargo Bay + Deployment)	24 to 44 °C (75.2 to 111.2 °F)
On-Orbit (On-Station)	23 to 45 °C (73.4 to 113 °F)
On-Orbit (Retrieval + Cargo Bay)	17 to 44 °C (62.6 to 111.2 °F)
Descent/Landing	13 to 43 °C (55.4 to 109.4 °F)
Post-Landing	13 to 43 °C (55.4 to 109.4 °F)
Ferry Flight	15.5 to 30 °C (59.9 to 86 °F)

Thermal Conditions	
USL module wall temperature	13 to 43 °C (55 to 109 °F)
JEM module wall temperature	13 to 43 °C (55 to 109 °F)
APM module wall temperature	13 to 43 °C (55 to 109 °F)
CAM module wall temperature	13 to 43 °C (55 to 109 °F)
Other integrated payloads racks	Front surface less than 37 °C (97 °F)

- Vibration

  - Vibration Environment

    The ISPR Rack shall meet the performance requirements specified herein after exposure, in its ascent configuration, to the random vibration environment defined in Table 3-II. (Ref. SSP 57000, Rev. B, Table 3.1.1.3-2)

TABLE 3-II RANDOM VIBRATION LAUNCH ENVIRONMENT

FREQUENCY	LEVEL
20 Hz	0.005 g^2/Hz
20-70 Hz	+5.0 dB/octave
70-200 Hz	0.04 g^2/Hz
200-2000 Hz	-3.9 dB/octave
2000 Hz	0.002 g^2/Hz
Composite	4.4 grms

Note: Criteria is the same for all directions (X, Y, Z)

- Acoustic

  - Acoustic Environment (Ref. SSP 41047, Part 1, Rev. C, Paragraph 3.2.1.4.1.1)

    The ISPR shall meet the performance requirements specified herein after exposure to the ascent acoustic environment defined in Table 3-III.

TABLE 3-III ACOUSTIC NOISE CRITERIA

1/3 Octave Band Center Frequency (Hz)	Sound Pressure Level (dB)	
	Liftoff (1)	Aeronoise (2)
31.5	111.5	96.0
40.0	93.5	99.5
50.0	98.0	102.0
63.0	102.5	105.0
80.0	114.0	108.0
100.0	124.0	110.0
125.0	122.0	112.0
160.0	121.0	113.5
200.0	124.5	115.0
250.0	123.0	116.0
315.0	121.5	116.5
400.0	121.5	114.5
500.0	117.0	111.0
630.0	115.5	107.5
800.0	114.5	104.5
1000.0	113.0	101.5
1250.0	109.0	97.5
1600.0	108.5	94.0
2000.0	106.0	90.0
2500.0	102.0	86.5
Overall	131.5	123.5

Notes:
(1) 5 seconds per mission (time per flight does not include a scatter factor)
(2) 10 seconds per mission (time per flight does not include a scatter factor)

- Acceleration

  - Transportation Acceleration Environment (Ref. SSP 57000, Rev. B, 3.1.1.1-D)

    The integrated ISPR Rack and its components shall meet the performance requirements specified herein after exposure to ground transportation accelerations of no more than 80% of the flight acceleration shown in Table 3-IV.

  - Flight Acceleration Environment (Ref. SSP 41017, Part 1, Rev. C, Paragraph 3.2.4.1.2 and SSP 57000, Rev. B, Paragraph 3.1.1.3.F)

    The ISPR Rack assembly shall meet the specified performance requirements after exposure, in its launch and landing configuration, to the launch and landing acceleration environments specified in Table 3-IV.

TABLE 3-IV RACK ASSEMBLY ACCELERATIONS

	Nx (g)	Ny (g)	Nz (g)	Rx* (rad/sec^2)	Ry* (rad/sec^2)	Rz* (rad/sec^2)
Launch	+/-7.0	+/-8.0	+/-7.8	+/-70.8	+/-21.7	+/-34.8
Landing	+/-5.3	+/-7.2	+/-9.0	+/-37.1	+/-23.0	+/-28.3
Ground Handling	+/-0.5	+/-1.0	+/-2.0	+/-0.0	0.0	0.0
On-Orbit	0.2 in any direction			N/A	N/A	N/A

*Rotation taken about Rack center of mass.

The ISPR Rack components shall meet the specified performance requirements after exposure, in its launch and landing configuration, to the launch and landing acceleration environments specified in Table 3-V.

TABLE 3-V RACK COMPONENT ACCELERATIONS

Liftoff	**x**	**y**	**z**
(g)	+/-7.7	+/-11.6	+/-9.9
Landing	**x**	**y**	**z**
(g)	+/-5.4	+/-7.7	+/-8.8

Note: Load factors apply concurrently in all possible combinations for each event and are shown in the rack coordinate system.

- Crew-Induced Loads (Ref. SSP 57000, Rev. B, Paragraph 3.1.1.3.D)

  The integrated rack equipment shall provide positive Margins of Safety when exposed to the crew-induced loads shown in Table 3-VI.

TABLE 3-VI CREW INDUCED LOADS

CREW SYSTEM OR STRUCTURE	TYPE OF LOAD	LOAD	DIRECTION OF LOAD
Personal Tether	Concentrated load (tension)	311.6 N (70 lbf), limit	Any direction
Personal Tether Attach Point	Concentrated load	1112.8 N (250 lbf), ultimate	Any direction
Handhold/Handrail Attach Points	Concentrated load at any point on the handhold/ handrail	1112.8 N (250 lbf), ultimate	Any direction
Foot Restraints	Concentrated load at the plate surface	445.1 N (100 lbf), limit	Any direction
	Moment	203.3N-M (150 ft-lbf), limit	Any direction
Levers, Handles, Operating Wheels, Controls	Push or Pull concentrated on most extreme edges	222.6 N (50 lbf), limit	Any direction
Small Knobs	Twist (torsion)	14.9 N-M (11 ft-lbf), limit	Either direction
Cabinets and any normally exposed equipment	Concentrated load applied by flat round surface with an area of ($0.093m^2$)($1 ft^2$)	556.4 N (125 lbf), limit 778.9 N (175 lbf), ult	Any direction
Legend: ft = feet, m = meter, N = Newton, lbf = pounds force			

- Safety Factors

  - Safety Factors (Ref. SSP 52005, Rev. B, Table 5.1.2-1)

    All Space Station Flight hardware structures shall be designed to the Factors of Safety specified in Table 3-VII. They are the factors which are to be used for payload flight structures mounted to primary and secondary structure.

TABLE 3-VII FACTORS OF SAFETY

	YIELD	ULTIMATE	PROOF
Metallic Structures			
- Untested Shuttle (analysis only)	1.25	2.0	-
- Untested on orbit (analysis only)	1.25	2.0	-
- Tested Shuttle (analysis and test)	1.0	1.4	1.2
- Tested on orbit (analysis and test)	1.1	1.5	1.2
Beryllium Structures			
- Static test and analysis		2.0	1.4
Composite Structures			
- Non-discontinuity Shuttle	-	1.4	1.2
- Non-discontinuity on orbit	-	1.5	1.2
-Discontinuity Shuttle	-	2.0	1.2
-Discontinuity on orbit	-	2.0	1.2
Ceramics & Glass			
- Static test & analysis (non-pressurized)	-	3.0	(accept.) 1.2
- Static test & analysis (pressurized)	-	3.0	(accept.) 2.0
- Analysis only (non-pressurized)	-	5.0	-
Structural Bonds			
- Bonded to glass (analysis and test)	-	2.0	(accept.) 1.2 (qual.) 1.4
-Other (analysis and test)	-	2.0	(accept.) 1.2

Note: "Shuttle" defines the transportation phases of the mission in the STS and "on orbit" defines operational activities in the ISS.

(This Page Intentionally Left Blank)

SECTION 4

MATERIAL PROPERTIES/ALLOWABLES

4.1 Metallic Material Specifications

The metallic materials used in the ISPR structure is given in Table 4-I. The material specifications for these materials is presented in each appropriate section.

TABLE 4-I METALLIC MATERIALS

Aluminum	CRES	Titanium	Misc. Material
2024-T62	A286	Ti-6A1-4V	MP35N
2219-T87	15-5PH		Nitronic 60
6061-T4	17-7PH		Inconel 718
6061-T6	304		
6061-T62			
6061-T651			
7075-T62			
7075-T73511			
7075-T7352			

- Non-Metallic Material Specifications

The following advance composite materials are used in the - ISPR construction:

1. Epoxy impregnated E-Glass fabric per D683-29042-1.
2. Epoxy impregnated unidirectional carbon fiber tape per D683-29519-1, Type 35, Class 2 (IM6/3501-6 tape).
3. Epoxy impregnated woven carbon fabric per D683-29042-1 (AS4/3501-6 fabric).

Both the unidirectional carbon tape and woven carbon fabric are used to form the primary load bearing structure of the ISPR. The E-Glass fabric is used as the outer most plies to form a corrosion barrier between the carbon/epoxy parts and the aluminum parts of the structure. The E-Glass does not contribute significantly to the strength or stiffness of the structure and therefore is not included in the ply lay-up used in the detail analysis.

The design allowables and properties used in the analysis of the composite structure are based on material properties and allowables developed for the Bell/Boeing V-22 Tilt Rotor aircraft program.

These allowables are the result of extensive notched laminate test and test/theory correlation utilizing the durability and damage tolerance criteria. The V-22 program tested various laminates in tension, compression, shear, bolt bearing and compression after impact in environments ranging from -65°F dry to +180°F wet environments. This data has been incorporated into the database of two Boeing developed composite analysis programs,

"INCAP" and "VLAM". These two programs are used to determine the laminate properties for a given lay-up.

(This Page intentionally Left Blank)

SECTION 5

LOADS

5.1 Introduction

The internal loads used in this analysis were generated using the MSC/NASTRAN finite element model of the CIR. The load factors for the integrated rack are taken from SSP 41017, Rack to MPLM ICD Part 1, Rev. C. There are 256 load cases if all of the load factor combinations for liftoff and landing are used together with hot and cold thermal cases. For this preliminary design analysis a subset of critical cases was selected by reviewing the ISPR analysis report and selecting twelve load cases that caused the lowest margins of safety. The thermal cases were analyzed separately and are documented in section 8.4. FEMAP post-processing software was used to determine the max /min values of internal load or strain.

Components are analyzed for a combination of component load factors and random vibration loads. The random vibration environment and the component load factors are specified in SSP 57000, Pressurized Payloads Interface Requirements Document, Rev. B. For this preliminary design analysis, a worst on worst combination of x, y, and z load factors was used in the analysis.

5.2 MPLM Launch & Landing Load Factors

The launch and landing load factors (accelerations) for the MPLM are specified in Table 3.2.1.4.2-1 of SSP 41017, Part 1, Rev. C. The load factors used in this analysis are summarized in Table 5-I. These load factors are for the integrated rack and represent a critical subset of all of the launch and landing cases.

There are separate load factors for component loads specified in SSP 57000, Rev. B, Paragraph 3.1.1.3.F. The component load factors are combined with the random vibration loads specified in SSP 57000, Rev. B, paragraph 3.1.1.3-2. The combined component/vibration loads were applied to the optical bench to calculate interface loads to the rack posts. They are summarized in Table 5-II. The maximum x, y, and z load factors were combined to make a worst on worst set.

TABLE 5-I LOAD CASES FOR THE INTEGRATED RACK

I.D.	Tx	Ty	Tz	Rx	Ry	Rz
101	+7.00	+8.00	+7.80	+70.8	+21.7	+34.8
102	+7.00	+8.00	-7.80	-70.8	+21.7	+34.8
103	-7.00	+8.00	+7.80	+70.8	-21.7	-34.8
104	-7.00	-8.00	+7.80	+70.8	-21.7	+34.8
105	+7.00	-8.00	+7.80	+70.8	+21.7	-34.8
106	+7.00	+8.00	-7.80	+70.8	-21.7	+34.8
107	+7.00	+8.00	+7.80	-70.8	-21.7	+34.8
108	-7.00	-8.00	+7.80	-70.8	+21.7	+34.8
109	-7.00	+8.00	+7.80	+70.8	-21.7	+34.8
110	+7.00	+8.00	-7.80	+70.8	+21.7	+34.8
111	-7.00	+8.00	+7.80	+70.8	+21.7	+34.8
112	-7.00	+8.00	-7.80	-70.8	+21.7	+34.8

TABLE 5-II COMPONENT LOAD CASES

I.D.	Tx	Ty	Tz	Rx	Ry	Rz
101	+12.5	+24.5	+21.1	0	0	0
102	+12.5	+24.5	-21.1	0	0	0
103	+12.5	-24.5	+21.1	0	0	0
104	+12.5	-24.5	-21.1	0	0	0
105	-9.5	+24.5	+21.1	0	0	0
106	-9.5	+24.5	-21.1	0	0	0
107	-9.5	-24.5	-21.1	0	0	0
108	-9.5	-24.5	+21.1	0	0	0

COMPONENT LOAD FACTOR CALCULATIONS

Input the component natural frequencies:

f_{nx} = 39.18 hz
f_{ny} = 81.99 hz
f_{nz} = 66.53 hz

SSP 57000-B, Table 3.1.1.3-2, Random Vibration Criteria ...

frequency		level	
20	hz	0.005	g^2/Hz
20 - 70	hz	5	db/oct
70 - 200	hz	0.04	g^2/Hz
200 - 2000	hz	-3.9	db/oct
2000	hz	0.002	g^2/Hz

Calculate the PSD levels from the above criteria: (Ref. SSP52005, Rev. B, Section 4.1.5.C)

PSDx = 0.015
PSDy = 0.040
PSDz = 0.037

$PSD_n = PDS_1 (f_n / f_1)^{3322s}$
Equation for charted numbers

Get the peak load factor using Miles' Equation

Rx = 9.20
Ry = 21.53
Rz = 18.61

$RLF = 3 * sqrt(\pi/2 * Q * f_n * PSD_n)$
Miles' Equation

Calculate the combined load factors:

LO1x = 12.5
LO1x = -9.5
LO2y = 24.5
LO3z = 21.1

Input calculated factors into the table: (Ref. SSP 52005, Rev. B, Table 4.1.2-1)

	Load Set	Orbiter X - Axis	Orbiter Y - Axis	Orbiter Z - Axis
Lift-Off	1	+ 12.5 -9.5	+ 11.6 - 11.6	+ 9.9 - 9.9
	2	+/- 7.7	+/- 24.5	+/- 9.9
	3	+/- 7.7	+/- 11.6	+/- 21.1
Landing	4	+/- 5.4	+/- 7.7	+/- 8.8

SECTION 6

CIR/ISPR FINITE ELEMENT MODELS

- Boundary Conditions

The ISPR rack assembly (including the knee brace assembly) is constrained at the knee brace to module wall connection and at the lower fittings to module wall connection.

The left knee brace strut, the right knee brace strut and the diagonal knee brace strut are constrained in the three translational directions at their attachment to the module wall. Appropriate pin releases are used in the knee brace assembly to accurately simulate the proper response of the knee brace assembly. Figure 6-1 shows the knee brace assembly, the constrained nodes and the constraint conditions.

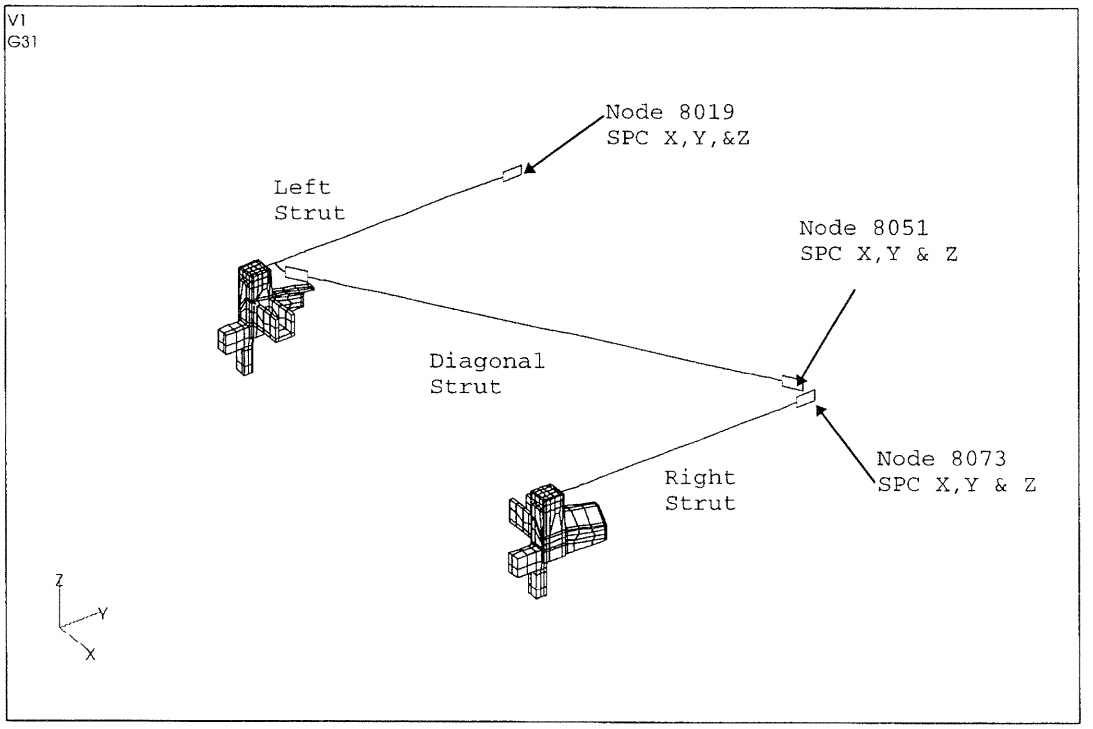

FIGURE 6-1 BOUNDARY CONDITIONS - KNEE

The lower left fitting is constrained in the three translation DOF's and the lower right fitting is constrained in the Y & Z directions. Figure 6-2 and 6-3 shows the Lower attach fittings, the constrained nodes and the constraint conditions.

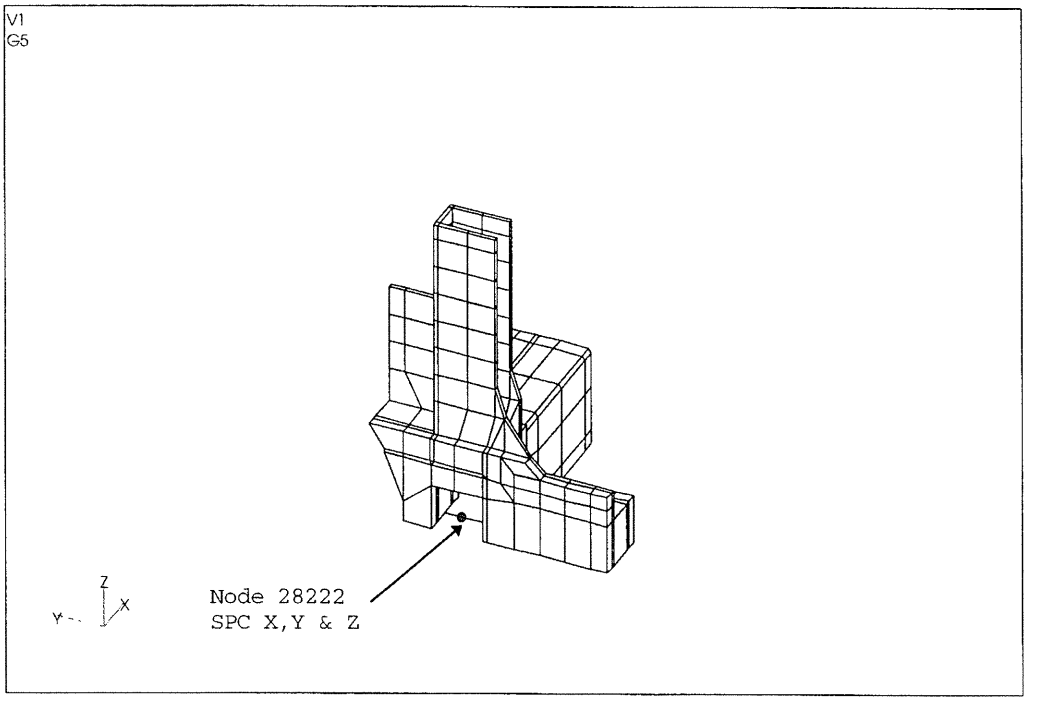

FIGURE 6-2 LOWER LEFT FITTING CONSTRAINT

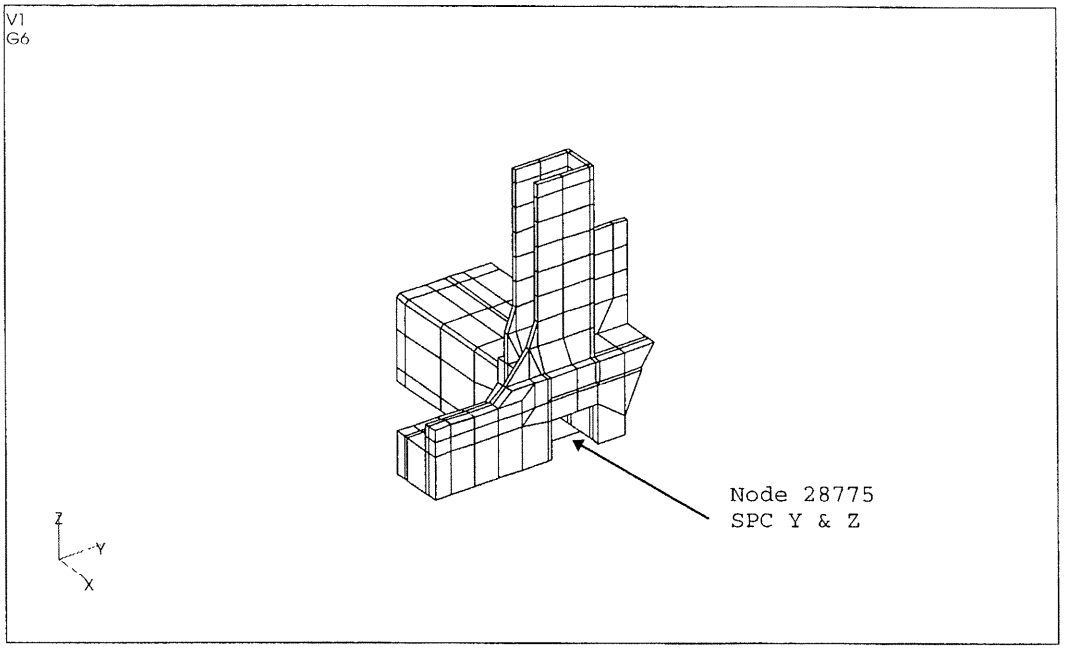

FIGURE 6-3 LOWER RIGHT FITTING CONSTRAINT

- Model Description

  The CIR finite element model is constructed as a combination of plate, solid, bar, rigid and spring elements. The CIR FEM (ISPR plus CIR payload) is shown in Figure 6-4.

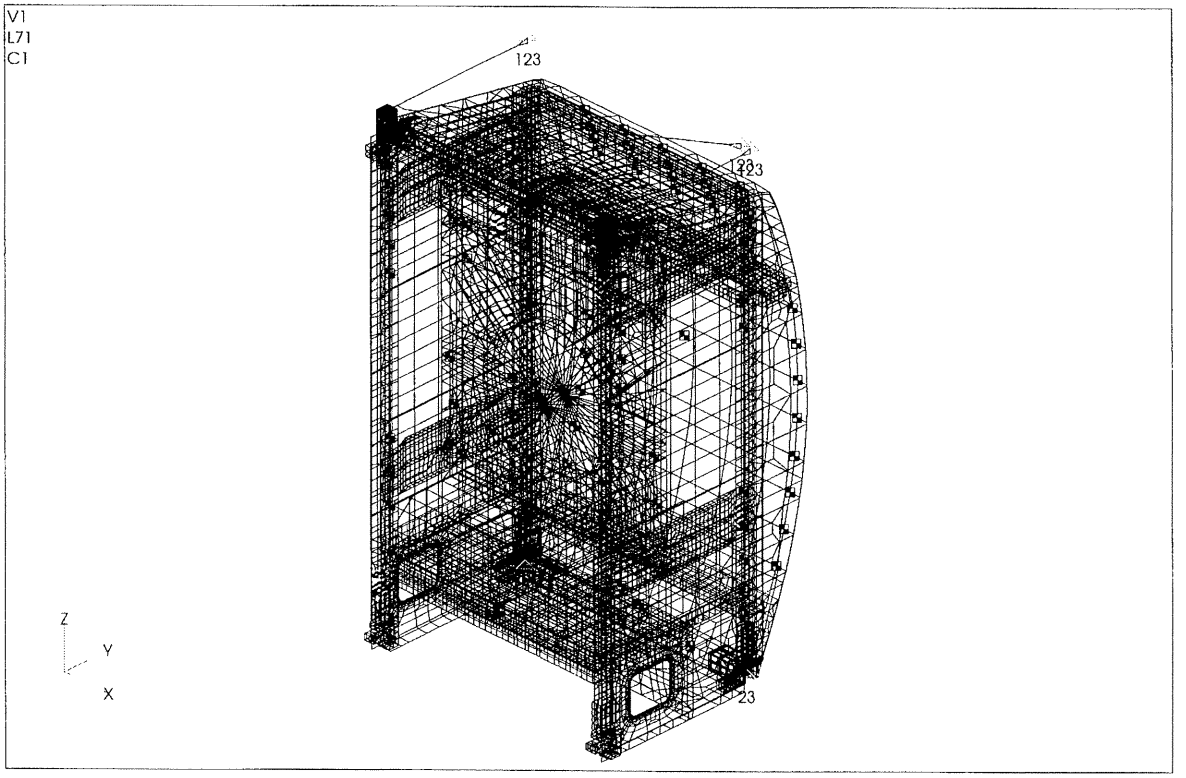

FIGURE 6-4 CIR FEM

Each of the separate components of the ISPR rack configuration is listed with the general modeling technique used to simulate that component.

- Skin Panels and Rear Access Panels

The skin is a single part made of epoxy impregnated carbon woven fabric with exterior plies of E-Glass. The lay-up varies from 10 to 22 plies and is quasi-isotropic for each ply stack. The rear access panels are simulated as a continuos piece of the skin. The skin and rear access panel portion of the ISPR FEM is shown in Figure 6-5. Skin and rear access panels are modeled with plate elements.

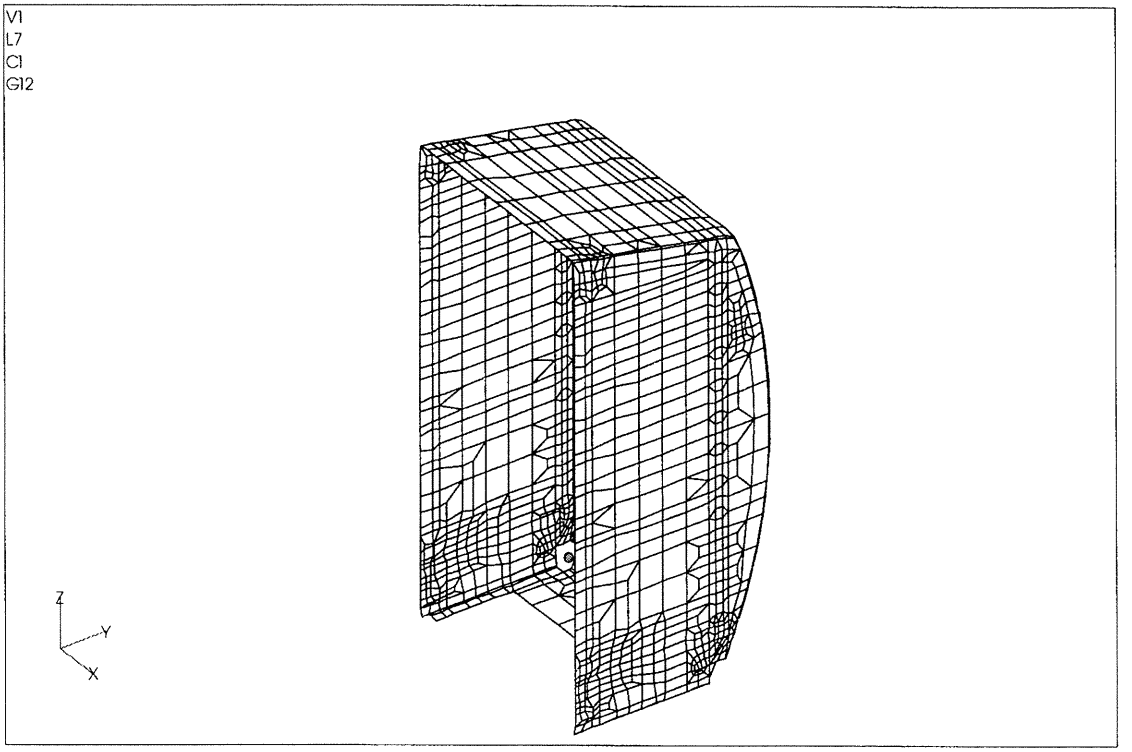

FIGURE 6-5 SKIN AND ACCESS PANELS

- Composite Posts

  The RSR posts are hybrid composite I-beams and are constructed as a combination or graphite tape and plain weave graphite fabric. The part is constructed of two channel sections and two caps which are combined in a hard tool to produce the resulting I-Beam. The skin to post fasteners are simulated as a combination of rigid and spring elements. The composite posts are modeled with plate elements. The composite posts of the ISPR FEM are shown in Figure 6-6.

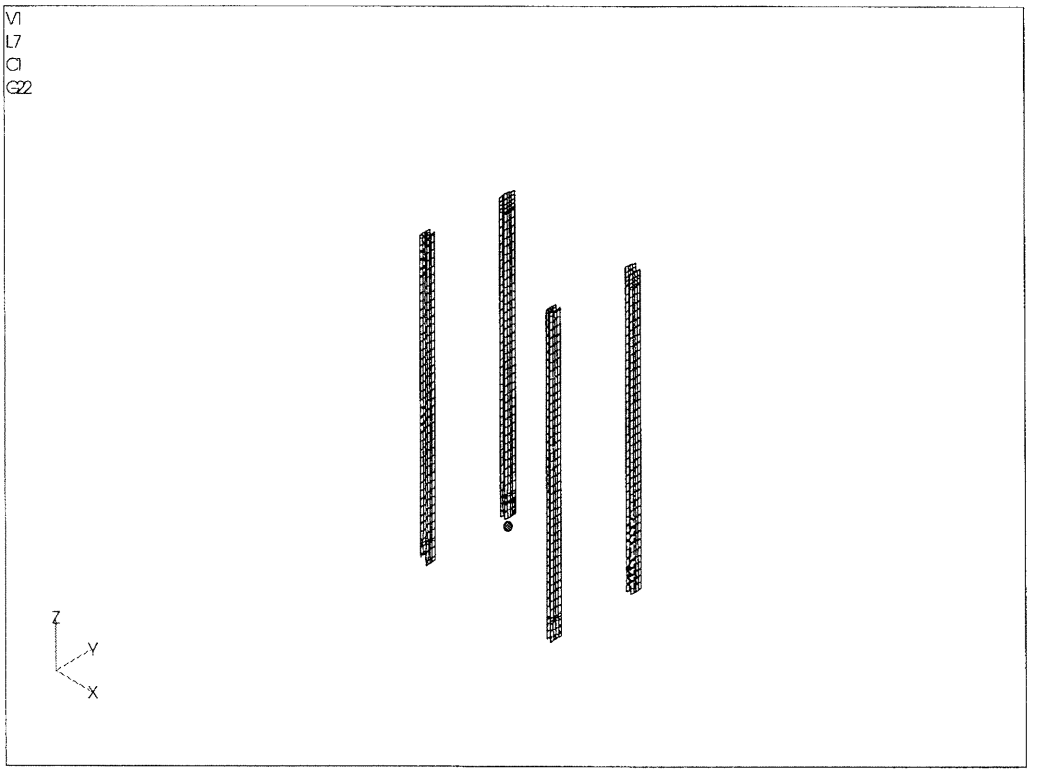

FIGURE 6-6 COMPOSITE POSTS

- Utility Panel Support Plate

  The utility panel support plate is a machined aluminum plate (Al. 7075-T7351). The utility panel support plate attaches to aluminum angles that attach to the composite side skin, the composite posts at the front, the horizontal beam, and the utility panel. Attachments (fasteners) are simulated by rigid/spring element combinations. The utility panel assembly is modeled with plate elements.

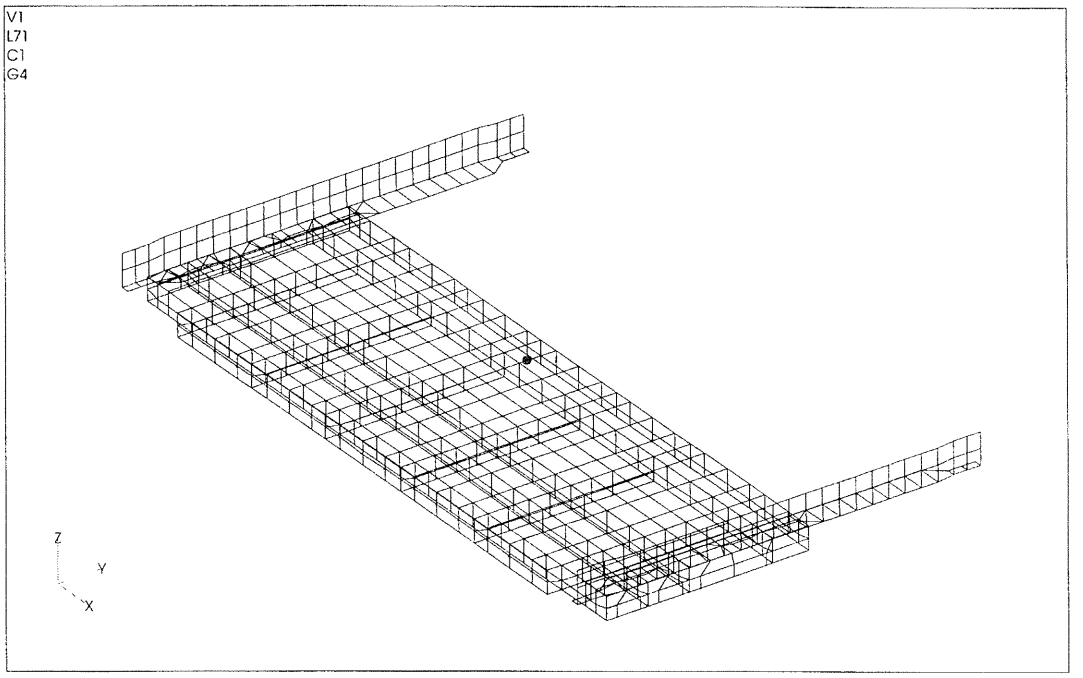

FIGURE 6-7 UTILITY PANEL SUPPORT PLATE

- Upper Torque Tubes

  The upper front torque tube (Al. 7075-T7351) connects to the upper left and upper right rack attach fittings. The upper rear torque tube attaches to the rear composite post by using two mounting clips (Al. 2219-T87). Additionally the stowage locker attaches to the front/rear torque tube at center span by way of a partiton fitting. The torque tubes are modeled with plate elements. All fasteners are simulated as a combination of rigid and spring elements.

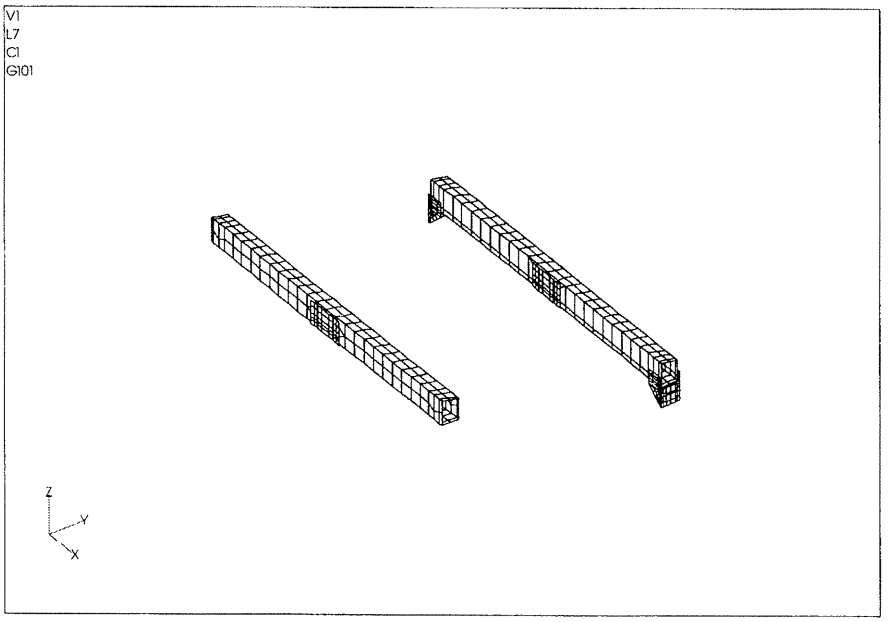

FIGURE 6-8 UPPER TORQUE TUBES, CLIPS AND PARTITION FITTINGS

- Lower Rear Horizontal Member

The lower rear horizonatl member (Al. 7075-T73) connects to the lower left and lower right rack attach fittings. Additionally it attaches to the rear and lower skin along it's full length.. The lower rear horizonatl member is modeled with plate elements. Attach fitting to horizontal member fasteners are simulated as a combination of rigid and spring elements. The attachment to the lower and rear skin is simulated by connecting to common nodes.

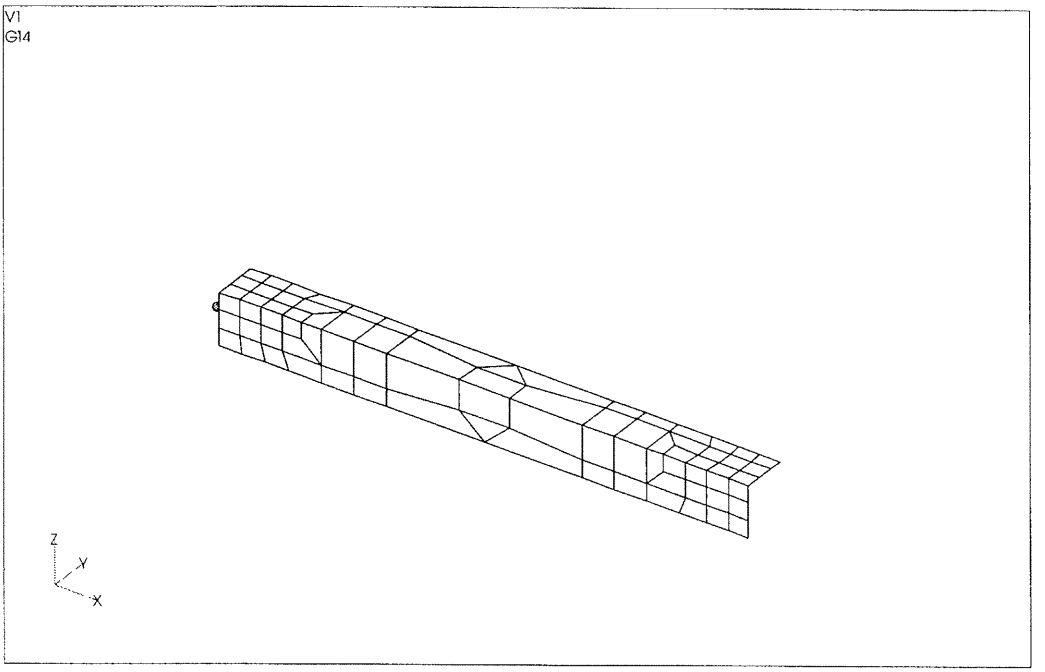

FIGURE 6-9 LOWER REAR HORIZONTAL MEMBER

- Upper Left/Right Attach Fittings

The upper attach fittings (Al. 7075-T7352) are dimensional identical and are mirror images of each other. The upper left attach fitting reacts load in the X and Y directions at the knee brace attachment and the upper right attach fitting reacts load in the Y direction only at the knee brace attachment. The X-direction flange attaches to the upper front torque tube, the Y-direction flange ties directly into the composite skin and the Z-direction flange is attached to the front composite posts. The upper attach fittings are modeled with a coarse mesh of solid elements. All fasteners are simulated as a combination of rigid and spring elements. Local models of the upper attach fittings were used in the analysis and are defined in their appropriate sections.

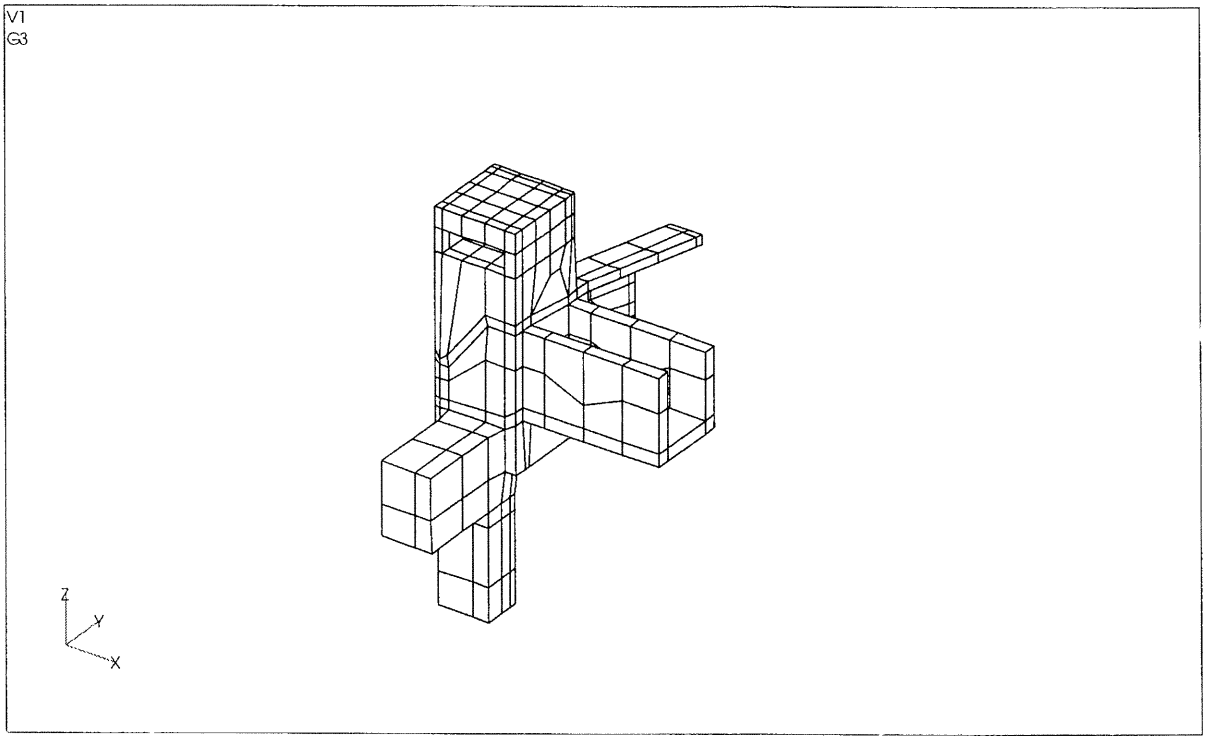

FIGURE 6-10 UPPER ATTACH FITTINGS

- Lower Left Attach Fittings

The lower left attach fitting (Ti - 6AL - 4V) ties directly to the module structure and reacts loads in all three translational directions. The X-direction flange attaches to the lower rear horizontal member, the Y-direction flange ties directly into the composite skin and the Z-direction flange is attached to the rear composite post. The clevis portion of the fitting (which is hidden in the following figure) attaches to the module wall via a module fitting. . The lower left attach fitting is modeled with a coarse mesh of solid elements. All fasteners are simulated as a combination of rigid and spring elements. A local model of the lower left attach fitting was used in the analysis and is defined in the appropriate section.

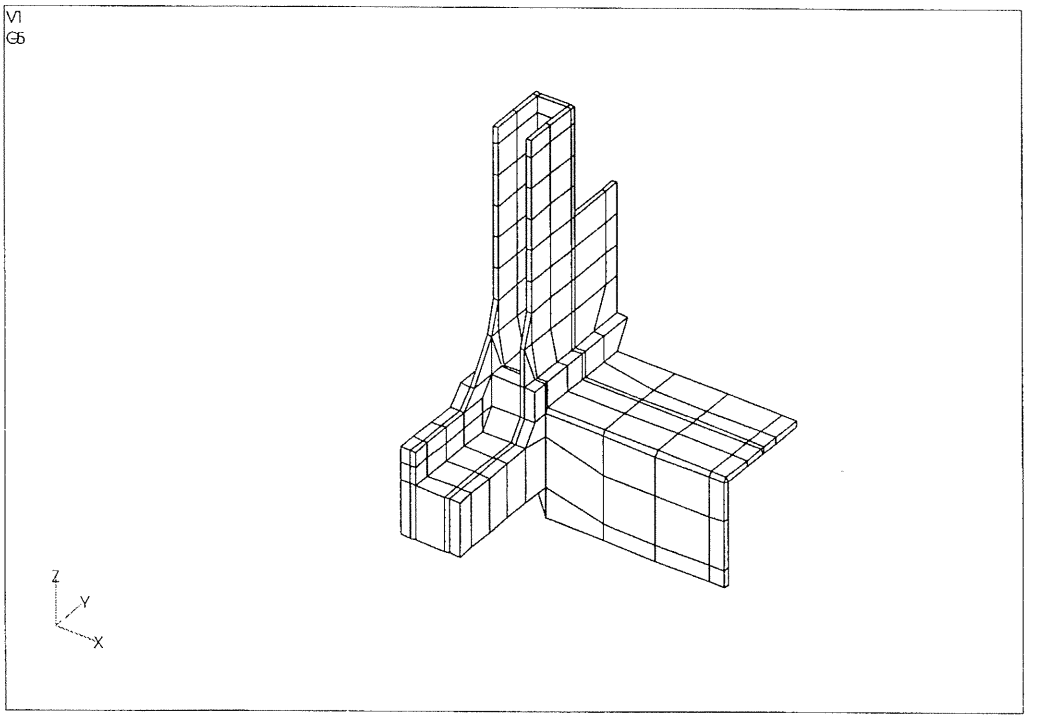

FIGURE 6-11 LOWER LEFT ATTACH FITTING

- Lower Right Attach Fittings

The lower right attach fitting (Al. 7075-T7352) ties directly to the module structure and reacts primary loads in the X and Z translational directions. Due to friction it reacts translational loads in the Y-direction. The X-direction flange attaches to the lower rear horizontal member, the Y-direction flange ties directly into the composite skin and the Z-direction flange is attached to the rear composite post. The clevis portion of the fitting attaches to the module wall via a module fitting. . The lower right attach fitting is modeled with a coarse mesh of solid elements. All fasteners are simulated as a combination of rigid and spring elements. A local model of the lower right attach fitting was used in the analysis and is defined in the appropriate section.

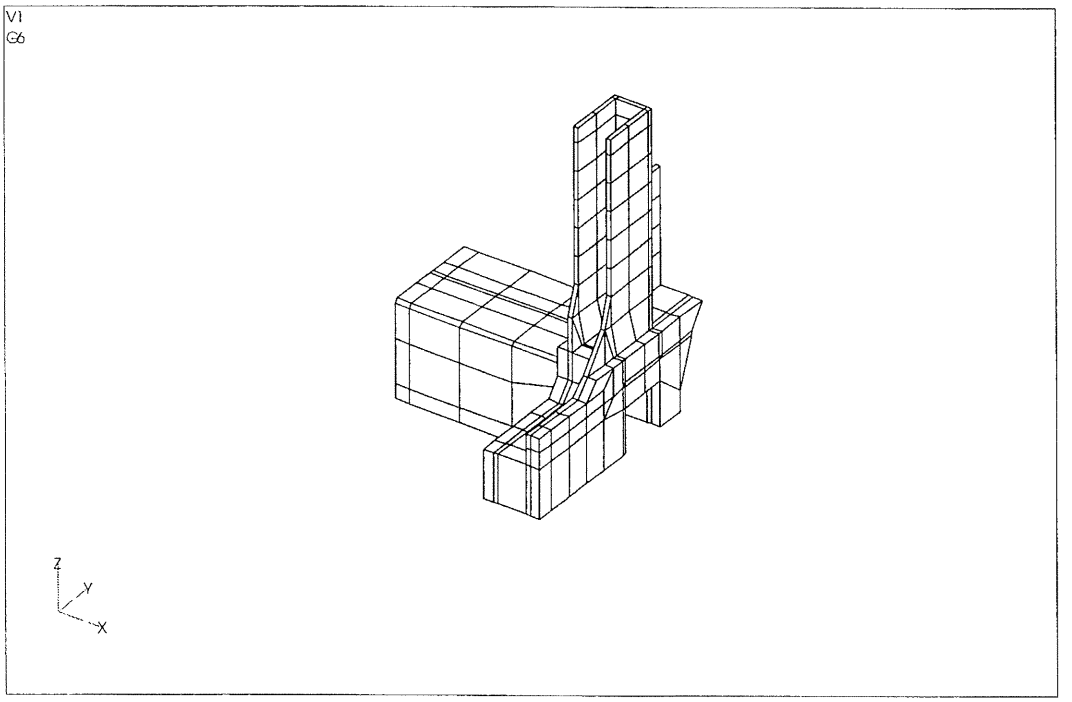

FIGURE 6-12 LOWER RIGHT ATTACH FITTINGS

- Pivot Fittings

The lower right and lower right attach fitting assemblies consists of the boss/lug potion (Ti-6AL-4V) and the flange portion (Al. 7075-T7351). They are located at the front lower region of the rack. The Z-direction flange attaches to the front composite posts. The clevis portion of the fitting attaches to the module stand-off assembly for on-orbit operations only. During a flight load event the pivot fittings are not constrained. The pivot fittings are modeled with a coarse mesh of solid elements. The pivot fittings are dimensionally identical. The lower left pivot is shown below. All fasteners are simulated as a combination of rigid and spring elements.

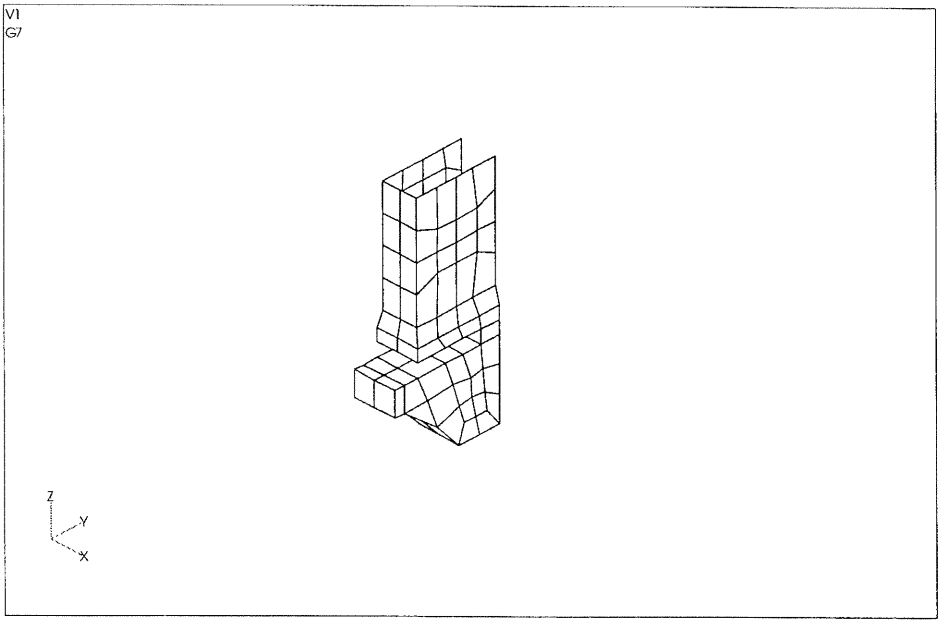

FIGURE 6-13 PIVOT FITTNGS

- Side Skin Stabilizers

  The RSR uses eight stabilizers, four on each side, to stiffen the skin. The six upper stabilizers (Al. 7075-T73) are simulated with bar elements. The two lower stabilizers (Al. 7075-T73) are simulated with plate elements. All stabilizers attach to the composite skin and to the front/rear composite posts. Their attachments to these structures are represented by using a combination of rigid and spring elements.

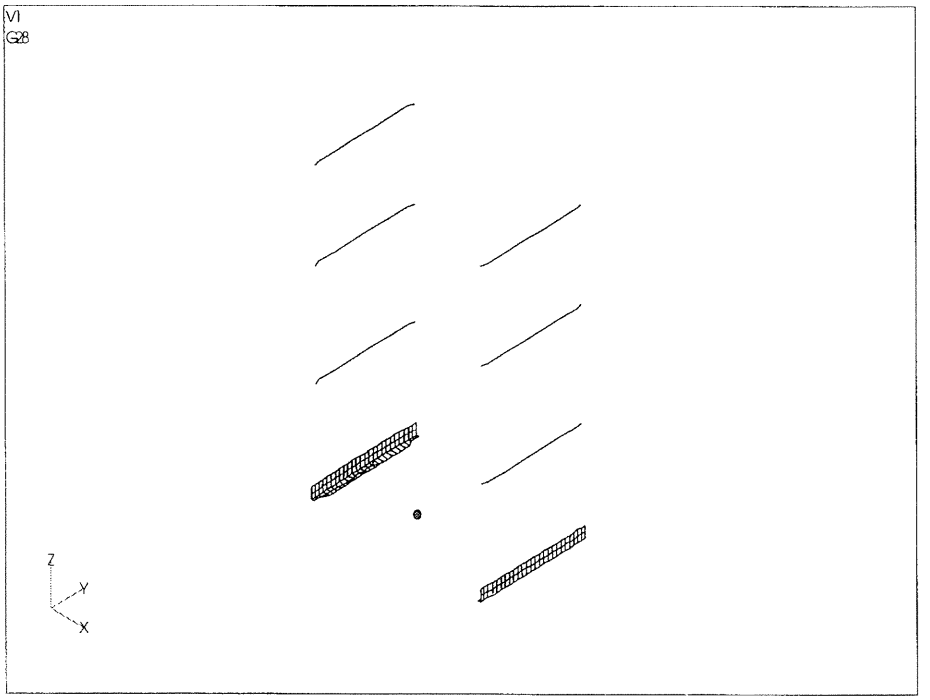

FIGURE 6-14 SIDE SKIN STABILIZERS

- Knee Brace Assembly

The knee brace assembly is not considered part of the ISPR assembly. However it must be represented in the analysis process to properly account for its effect on the load distribution during flight. The knee brace assembly attaches to the upper right and upper left attach fitting on the rack side and to the module wall. It is modeled with bar elements with pin releases to properly simulate the boundary conditions.

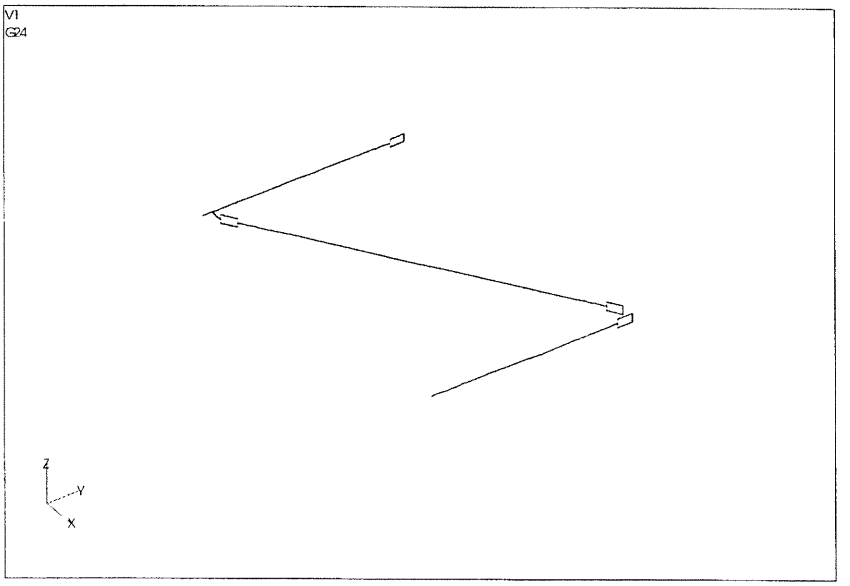

FIGURE 6-15 KNEE BRACE ASSEMBLY

- MODEL CHECK OUT PROCEDURES

The CIR finite element model was exposed to two standard check-out procedures to verify model response. Each procedure was succesfully completed with the following result.

1) Rigid Body Check

A normal modes solution was run for the CIR dynamic model in a free-free condition with the knee brace assembly constrained against rigid body motion. Six rigid bodies modes were obtained.

2) Enforced Displacement Solution

A static solution with enforced displacements was run for the CIR dynamic model and stress model. A translational enforced displacement was run in the three coordinate directions x,y and z. There should be no strain in the model for this condition, however strains were present in the payload. The source was traced to QUAD8 elements used in a mesh transition area with elements attached to the midside nodes. The QUAD8 elements were replaced with TRIA3 and QUAD4 elements and the solution was rerun. With this modification the model is strain free for rigid body displacements.

- MODEL MASS PROPERTIES

The integrated model has a weight of 1554.2 pounds. The center of gravity is located at (x, y, z) = (19.09, -11.47, 36.38).

SECTION 7

DYNAMIC MODEL

A dynamic finite element model of the CIR was prepared to calculate frequencies and normal modes for the CIR. This is to satisfy the requirement for a first fundamental frequency of 25 hz for the integrated rack. The dynamic model of the CIR was prepared by removing the payload from the stress model prepared by NASA Lewis personnel and adding it to the ISPR dynamic model. Note that the payload model was slightly modified to remove the QUAD8 elements. These elements had been used to provide a transition in the mesh. This technique introduces artificial constraints. The QUAD8 elements were replaced with a combination of QUAD4 and TRIA3 elements. The dynamic model that was used in this analysis is the dynamic model of the ARIS equipped ISPR. The NASTRAN file is named "CIR_aris_dyn_3.NAS" and is stored on the Boeing Huntsville computer system.

The integrated dynamic model is shown in Figure 7-1.

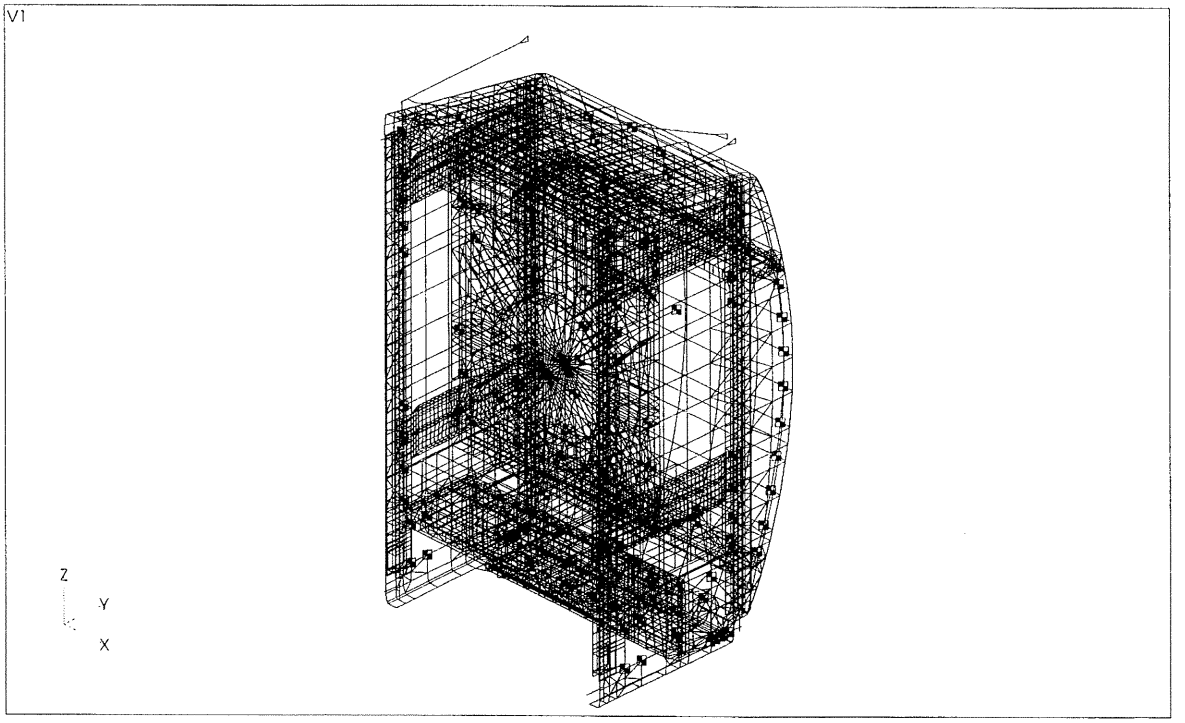

FIGURE 7-1 CIR DYNAMIC MODEL

A free-free run was made as a check of rigid body modes. The kneebraces were constrained against rigid body rotation. There are six rigid body modes for the integrated model, as expected. An enforced displacement solution was also run to check for grounding. The model is stress free for rigid body displacements.

A normal modes solution was run with the rack and kneebraces constrained at the interfaces that represent the module wall. The constraints consist of x, y, z constraints at the kneebraces and lower left fitting and y, z constraints at the lower right fitting. The results are shown in Table 7-I.

Mode 1 is the rack post bending mode, which is typical and is shown in Figure 7-2. The frequency of the first mode is 25.3 hz which satisfies the 25 hz requirement.

TABLE 7-I NORMAL MODES

REAL EIGENVALUES

MODE NO.	EXTRACTION ORDER	EIGENVALUE	RADIANS	CYCLES	GENERALIZED MASS	GENERALIZED STIFFNESS
1	1	2.53E+04	1.59E+02	2.53E+01	1.00E+00	2.53E+04
2	2	4.61E+04	2.15E+02	3.42E+01	1.00E+00	4.61E+04
3	3	6.19E+04	2.49E+02	3.96E+01	1.00E+00	6.19E+04
4	4	7.30E+04	2.70E+02	4.30E+01	1.00E+00	7.30E+04
5	5	7.88E+04	2.81E+02	4.47E+01	1.00E+00	7.88E+04
6	6	9.44E+04	3.07E+02	4.89E+01	1.00E+00	9.44E+04
7	7	9.82E+04	3.13E+02	4.99E+01	1.00E+00	9.82E+04
8	8	1.00E+05	3.17E+02	5.04E+01	1.00E+00	1.00E+05
9	9	1.04E+05	3.22E+02	5.13E+01	1.00E+00	1.04E+05
10	10	1.06E+05	3.25E+02	5.18E+01	1.00E+00	1.06E+05

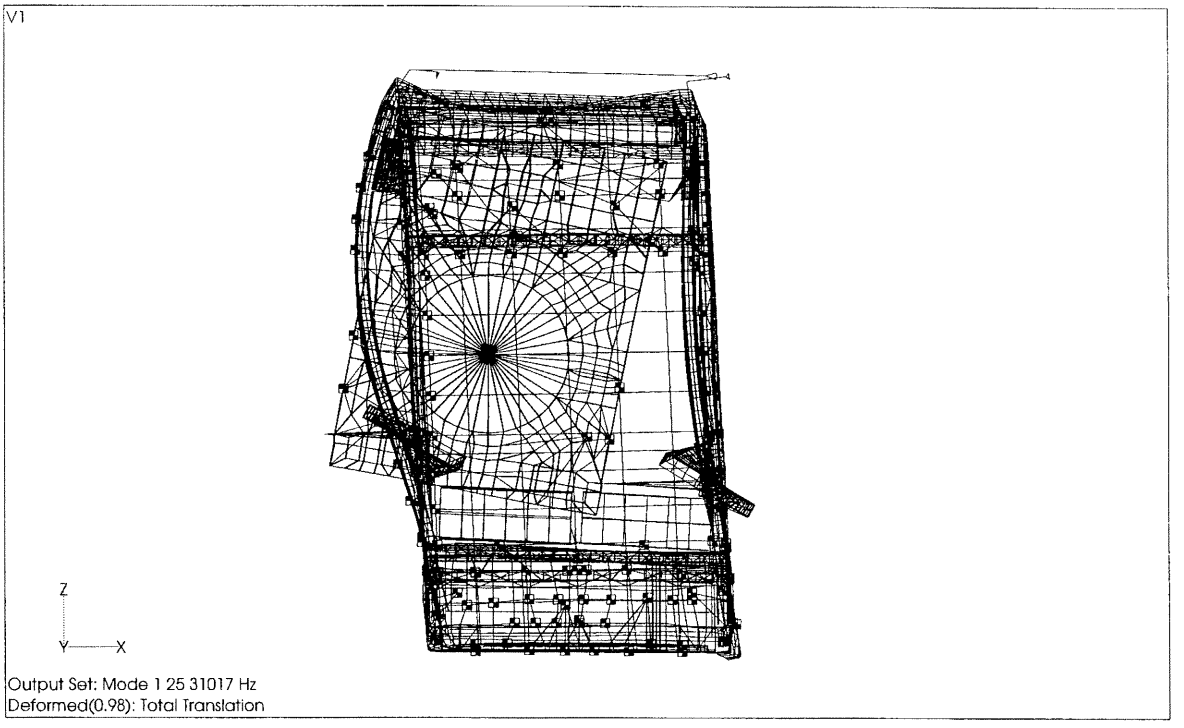

FIGURE 7-2 CIR MODE 1

The normal modes of the optical bench are required in order to calculate the random vibration loads. The optical bench normal modes were calculated with the optical bench constrained at the payload to post interface. The results are summarized below.

Table 7-II OPTICAL BENCH REAL EIGEN VALUES

MODE NO.	EXTRACTION ORDER	EIGENVALUE	RADIANS	CYCLES	GENERALIZED MASS	GENERALIZED STIFFNESS
1	1	6.06E+04	2.46E+02	3.92E+01	1.00E+00	6.06E+04
2	2	1.75E+05	4.18E+02	6.65E+01	1.00E+00	1.75E+05
3	3	2.65E+05	5.15E+02	8.20E+01	1.00E+00	2.65E+05
4	4	5.85E+05	7.65E+02	1.22E+02	1.00E+00	5.85E+05
5	5	6.26E+05	7.91E+02	1.26E+02	1.00E+00	6.26E+05
6	6	1.03E+06	1.01E+03	1.61E+02	1.00E+00	1.03E+06
7	7	1.07E+06	1.04E+03	1.65E+02	1.00E+00	1.07E+06
8	8	1.38E+06	1.17E+03	1.87E+02	1.00E+00	1.38E+06
9	9	2.37E+06	1.54E+03	2.45E+02	1.00E+00	2.37E+06
10	10	2.45E+06	1.56E+03	2.49E+02	1.00E+00	2.45E+06

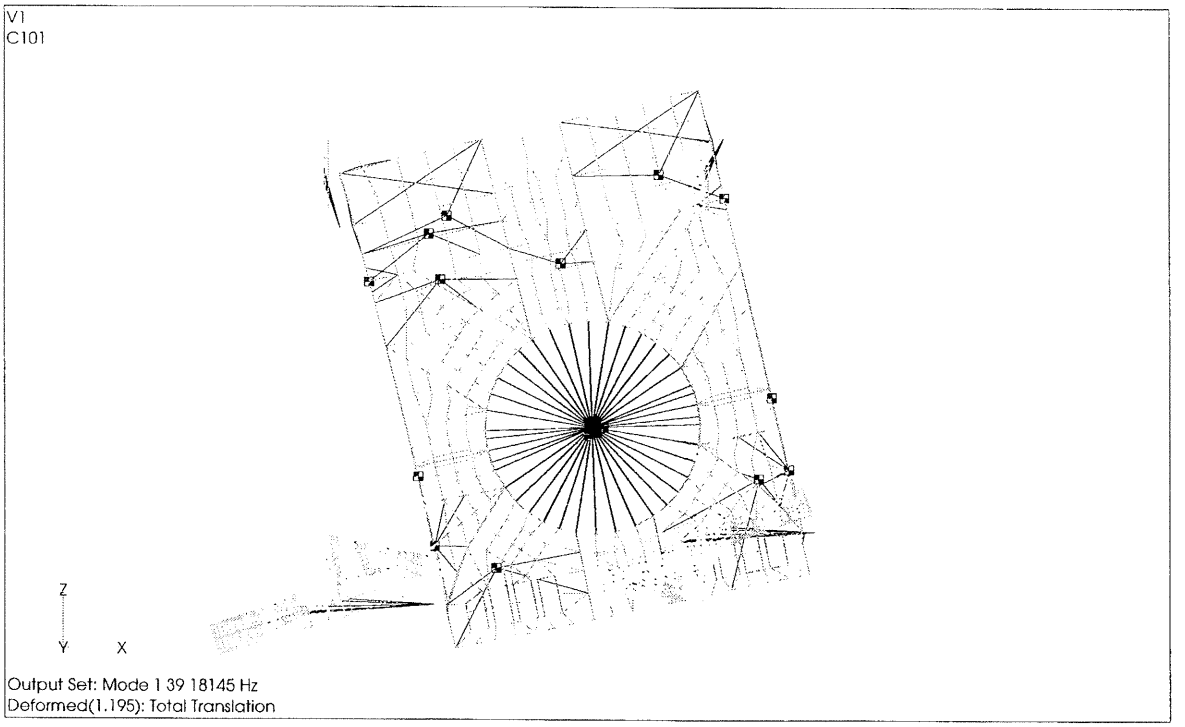

FIGURE 7-3 OPTICAL BENCH X MODE

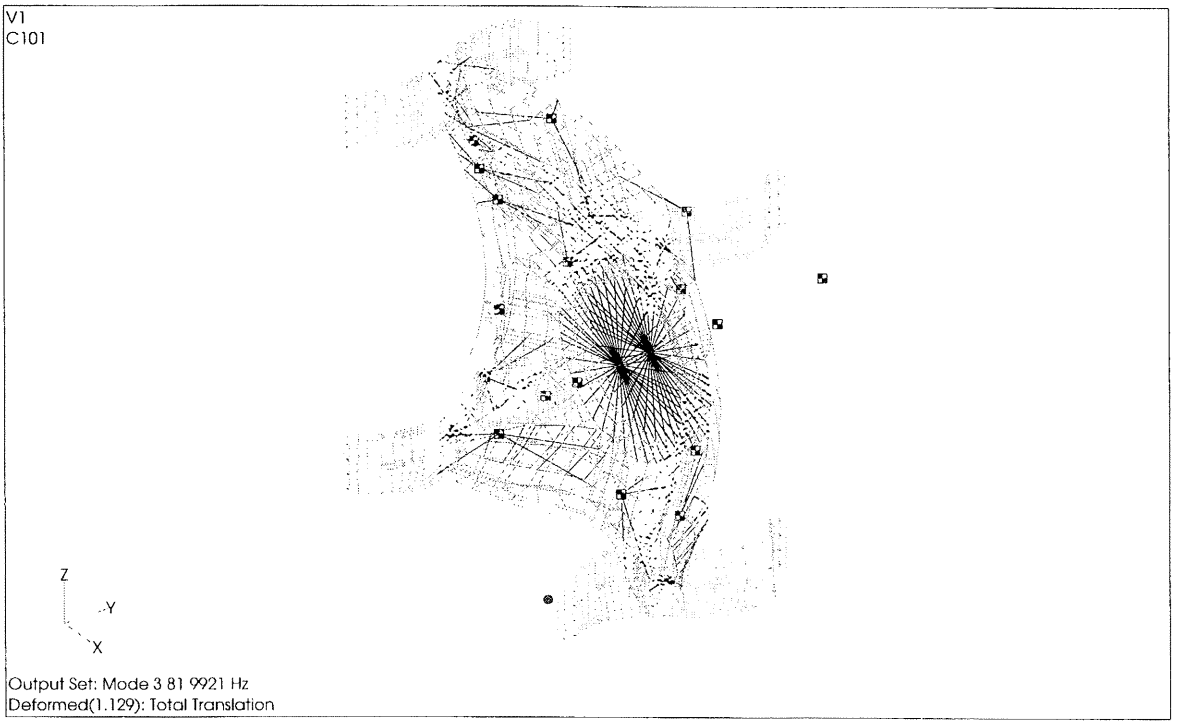

FIGURE 7-4 OPTICAL BENCH Y MODE

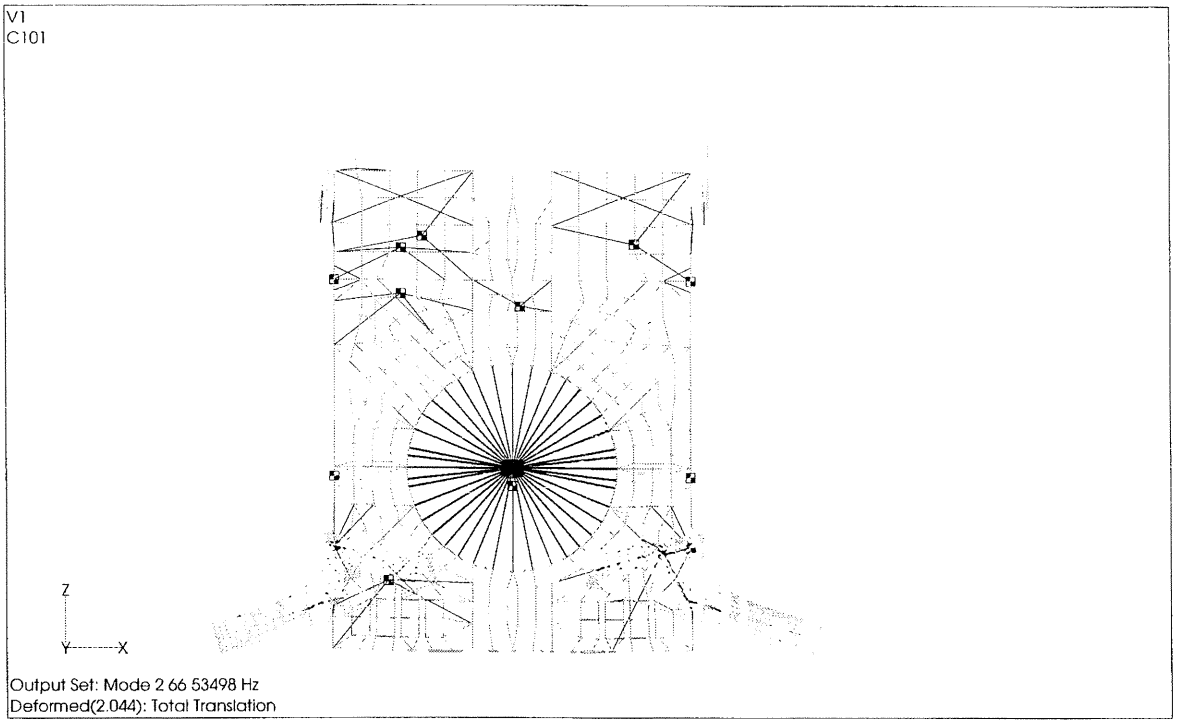

FIGURE 7-5 OPTICAL BENCH Z MODE

(This Page Intentionally Left Blank)

SECTION 8

STRUCTURAL ANALYSIS

8.1 Attach Fittings

The basic analysis of this component is detailed in section 8.3 of Ref. D683-30037-3 and section 8.8 of D683-30037-6. From this analyses, the Upper Left Attach Fitting is critical. All load cases producing maximum absolute values of reaction and interface load were investigated. The modeling techniques, material properties, and component geometry are identical to those presented in Ref. D683-30037-6.

RACK ACCELERATIONS
(Ref. SSP 41017, Table 3.2.1.4.2-1)

	Nx (g)	Ny (g)	Nz (g)	Rx (r/s^2)	Ry (r/s^2)	Rz (r/s^2)
Launch	± 7.0	± 8.0	± 7.8	± 70.8	± 21.7	± 34.8
Landing	± 5.3	± 7.2	± 9.0	± 37.1	± 23.0	± 28.3
HDL.	± 0.05	± 1.0	+ 2.0/0.0	0.0	0.0	0.0
Orbit	0.02	0.02	0.02	N/A	N/A	N/A

By solving for unit accelerations in all degrees of freedom and examining reaction signs, maximum reaction and interface combinations can be formed. Note that essentially all loads are ±, therefore all reaction/interfaces are ± and all stress are ±, and therefore reported without sign. By inspection and previous analyses,

CONTROLLING LOADCASE, LAUNCH

Nx	Ny	Nz	Rx	Ry	Rz
± 7.0 g	± 8.0 g	± 7.8 g	± 70.8 r/s^2	± 21.7 r/s^2	± 34.8 r/s^2

RACK INTERFACE POINTS INVESTIGATED
(Ref. FEM Model CIR MPC3) Set 6

Set 6 = 8019, 8051, 8073, 28222, 28775 = Rack Interface Point (i.e., Reactions)

MAXIMUM REACTIONS FROM SPC FORCES, CIR ALL FEM MODEL

COMP	CASE	VALUE (lbs)
8019 x	102	24.07
8019 y	103	7226.4
8019 z	101	10.92
8051 x	103	4862.4
8051 y	102	3153.2
8051 z	102	22.53
8073 x	104	10.99
8073 y	107	6037.7
8073 z	102	10.89
28222 x	108	7123.3
28222 y	108	5952.0
28222 z	105	8588.0
28775 x	-	0
28775 y	110	4834.4
28775 z	109	8295.8

All load cases were investigated and mapped to detailed fitting models. Values are shown here for convenience. Displacements are used to map from gross FEMS to detailed FLGX and FLGY models.

Critical load cases are identified by using FEMAP to search for and identify high stress.

The detail FLGX and FLGY models are shown in Figures 8.1-1 and 8.1-2. Maximum stresses are summarized in Tables 8.1-I and 8.1-II.

Resulting stresses, allowable, factors of safety and Margins of Safety are summarized below.

X- and Y-Flanges

Material = Aluminum Alloy -7075-T7352 (Ref. Section 8.3 of D683-30037-2)

	F_{TY} (ksi)	F_{TU} (ksi)	FS_Y	FS_U	fvm (ksi)
X-FLG	43.4	57.0	1.0	1.4	28.453
Y-FLG	43.4	57.0	1.0	1.4	28.759

Note: M.S. = F/f(FS) - 1

X-FLG: $M.S._Y = 43.4./28.453 - 1 = \underline{0.53}$

$M.S._U = 57.0./(28.453 \times 1.4) - 1 = \underline{0.43}$

Y-FLG: $M.S._Y = 43.4./28.759 - 1 = \underline{0.52}$

$M.S._U = 57.0./(28.759 \times 1.4) - 1 = \underline{0.42}$

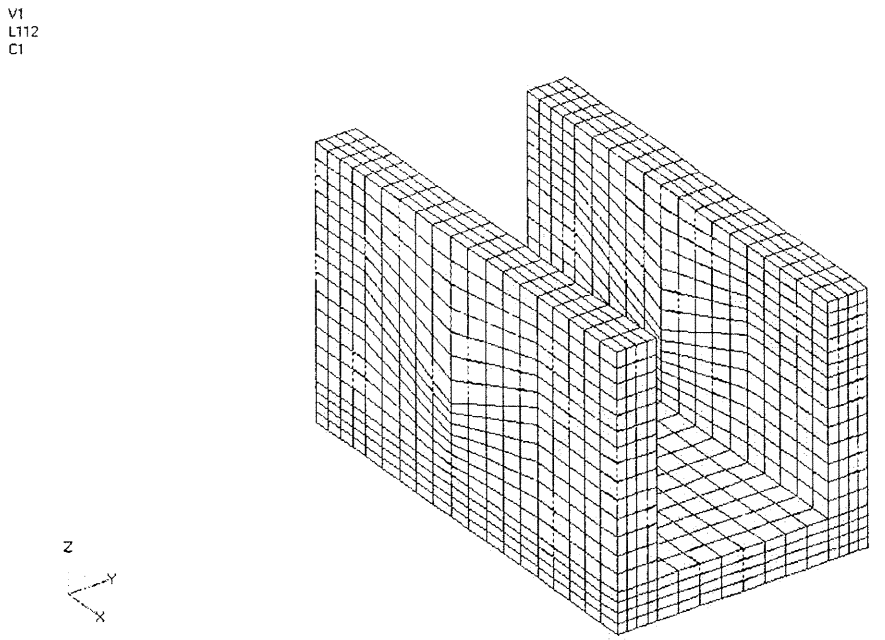

FIGURE 8.1-1 DETAIL FEM, UPPER LEFT ATTACH FITTING, X-FLANGE

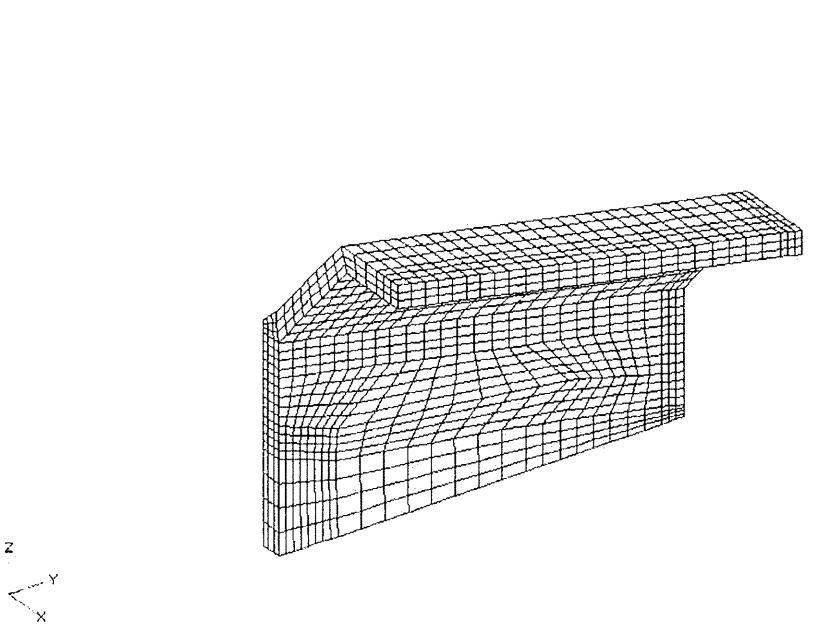

FIGURE 8.1-2 DETAIL FEM, UPPER LEFT ATTACH FITTING, Y-FLANGE

TABLE 8.1-I MAXIMUM STRESS SUMMARY, UPPER LEFT ATTACH FITTING, X-FLANGE

Final	MAX/MIN Summary Table	Set	ID	VALUE
Solid X Normal Stress	Min	4	2400	-29854.3
	Max	1	2400	31204.1
Solid XY Shear Stress	Min	4	2400	-2378.15
	Max	3	436	2447.15
Solid Max Prin Stress	Min	4	2400	-5929.71
	Max	2	2400	35686.7
Solid DirCos 11 Stress	Min	4	424	-0.16
	Max	5	2408	0.99
Solid DirCos 12 Stress	Min	1	2416	-0.14
	Max	3	2408	0.98
Solid DirCos 13 Stress	Min	3	452	-0.59
	Max	7	2420	0.33
Solid Mean Stress	Min	2	2400	-16825.0
	Max	4	2400	16409.2
Solid VonMises Stress	Min	7	428	8558.5
	Max	2	2400	28453.2
Solid Y Normal Stress	Min	4	2400	-6317.8
	Max	1	2400	6141.37
Solid YZ Shear Stress	Min	3	436	-2166.35
	Max	5	436	2032.69
Solid Min Prin Stress	Min	4	2400	-34397.2
	Max	1	2400	5836.75
Solid DirCos 21 Stress	Min	12	448	-0 26
	Max	3	2400	1.0
Solid DirCos 22 Stress	Min	7	428	-0.4
	Max	2	2404	1.0
Solid DirCos 23 Stress	Min	1	432	-1.0
	Max	12	2412	0.41
Solid Z Normal Stress	Min	4	2400	-13055.6
	Max	2	2400	13454.0
Solid ZX Shear Stress	Min	2	2400	-9810.2
	Max	4	2400	9463.23
Solid Int Prin Stress	Min	4	2400	-8900.85
	Max	2	2400	9137.91
Solid DirCos 31 Stress	Min	5	452	-0.65
	Max	4	432	0.96
Solid DirCos 32 Stress	Min	3	452	-0.63
	Max	1	432	0.96
Solid DirCos 33 Stress	Min	3	2408	-0.98
	Max	2	2420	0.39

TABLE 8.1-II MAXIMUM STRESS SUMMARY, UPPER LEFT ATTACH FITTING, Y-FLANGE

Final	MAX/MIN Summary Table	Set	ID	VALUE (PSI)
Solid X Normal Stress	Min	2	398	-7794.51
	Max	4	398	8512.36
Solid XY Shear Stress	Min	4	398	-6137.14
	Max	7	398	6237.35
Solid Max Prin Stress	Min	5	406	-5953.5
	Max	4	398	34535.1
Solid DirCos 11 Stress	Min	7	2586	-0.67
	Max	5	478	1.0
Solid DirCos 12 Stress	Min	8	398	-0.59
	Max	3	478	1.0
Solid DirCos 13 Stress	Min	7	414	-1.0
	Max	11	406	0.7
Solid Mean Stress	Min	4	398	-15796.7
	Max	2	398	15658.2
Solid VonMises Stress	Min	8	2490	4362.84
	Max	2	398	28758.6
Solid Y Normal Stress	Min	2	398	-33633.9
	Max	4	398	33045.5
Solid YZ Shear Stress	Min	12	2546	-6158.89
	Max	5	2642	5325.74
Solid Min Prin Stress	Min	2	398	-34783.2
	Max	3	406	7510.52
Solid DirCos 21 Stress	Min	8	2466	-0.69
	Max	2	1126	1.0
Solid DirCos 22 Stress	Min	2	2466	-0.68
	Max	1	414	1.0
Solid DirCos 23 Stress	Min	3	2370	-0.57
	Max	1	2490	0.35
Solid Z Normal Stress	Min	2	2634	-8493.44
	Max	3	406	7914.01
Solid ZX Shear Stress	Min	5	1078	-1438.87
	Max	12	2546	1590.11
Solid Int Prin Stress	Min	2	2634	-8430.51
	Max	3	406	8304.14
Solid DirCos 31 Stress	Min	4	2466	-0.69
	Max	1	406	0.99
Solid DirCos 32 Stress	Min	1	2466	-0.67
	Max	7	486	0.99
Solid DirCos 33 Stress	Min	1	2514	-1.0
	Max	8	406	0.66

Y-Flange to Skin

Reference D683-30037-3, 8.14-14 thru 8.14-18.

Conservatively assume Max Fastener loads $\leq$ Max Fastener Constraint Force from FEM Analysis. (FLYFAST.NAS Model) Examination of the distribution of the FEM Constraint

Forces to fasteners verifies this assumption. Maximum FEM Constraint forces are summarized in Table 8.1-III. The Node 26097 Force under load case 5 is identified as the maximum case. Complete Constraint Forces for case 5 are shown in Table 8.1-IV.

The worst case fastener load is:

$$Pfast = \sqrt{T1^2 + T2^2 + T3^2}$$

$$= \sqrt{40.8^2 + 241.3^2 + 999.5^2}$$

$$= 1029 \text{ lbs}$$

From D683-30037-3, Fbru = 2095 lbs.

M.S. = Fbru/(2 x Pfast) - 1 = 2095/2058 - 1 = $\underline{\underline{+0.02}}$

TABLE 8.1-III MAXIMUM CONSTRAINT FORCE SUMMARY

CONSTRAINT	FORCE	SET	ID	VALUE (LBS)
T1	Minimum	4	26359	-486.186
T1	Maximum	2	26359	519.126
T2	Minimum	4	26363	-536.448
T2	Maximum	7	26363	736.965
T3	Minimum	12	26097	-940.293
T3	Maximum	5	26097	999.646

TABLE 8.1-IV FORCES OF SINGLE-POINT CONSTRAINT (LBS)

POINT ID.		T1	T2	T3
26361	G	1.357309E+2	-2.863626E+2	7.588068E+1
26363	G	-4.970490E+1	-3.700007E+2	1.570849E+2
26359	G	4.100395E+2	-2.855029E+2	5.485585E+1
26093	G	2.969094E+1	-2.828331E+2	5.690499E+2
26097	G	-4.080165E+1	-2.412800E+2	9.996461E+2

8.2 Forward and Aft Posts

8.2.1 Introduction

There are four graphite epoxy posts in the ISPR that provide the payload attachment points. The post has an "I" beam cross section. Two checks are made for the posts. The first check is for strain in the post caps and webs due to the integrated rack load factors. This analysis is presented in section 8.2.2.

The second check of the posts is a local check of the post noodle region which is presented in section 8.2.3. The noodle is located at the intersection of the post cap and web. This critical loading at this location is due to payload to post interface loads. Two sets of load cases were analyzed. The first set of load cases are the same loads factors used in section 8.2.1. The second set of load cases are the component loads. The load factors for components are larger than the integrated rack load factors. In addition the component loads include a contribution from random vibration. A conservative set of worst on worst load factors were used for the component loads analysis. This resulted in negative margins of safety. A more detailed analysis should result in positive margins of safety for this location. The analysis presented here is adequate for a preliminary design analysis and highlights an area that should be carefully monitored during detail design. A detailed analysis will be included in the final report.

A fastener analysis is presented in section 8.2.4. Both integrated rack loads and component loads were analyzed. The component loads show a negative margin of safety in bearing. A more detailed analysis with less conservative component loads should result in a positive margin of safety.

8.2.2 Post Analysis

TABLE 8.2.2-I POST WEB ELEMENT PRINCIPAL STRAINS SUMMARY

	TOP		BOTTOM	
CASE	ϵ_{MAX} (μ in/in)	ϵ_{MIN} (μ in/in)	ϵ_{MAX} (μ in/in)	ϵ_{MIN} (μ in/in)
101	1705	-887	866	-1753
102	2106←	-851	946	-1809
103	1784	-843	976	-1924
104	880	-1913	1715	-871
105	992	-1969←	1814←	-1318
106	1762	-1078	887	-1567
107	1893	-826	918	-1850
108	961	-1927	1771	-944
109	1882	-900	898	-2078
110	1739	-976	971	-1580
111	1973	-865	757	-2121←
112	1850	-849	1171	-1767

Max ϵ_{SF} = 2121 μ-in/in (ϵ_{MIN}, bottom, case 111)

EL = 21416

ϵ_{ULT} at Surface = ϵ_{US} = 1.3(0.003426) [Ref. D683-30037-3, 8.2.1-12]

= 4453.8 μ-in/in

$$M.S._{ULT} = \frac{\epsilon_{ULT}}{\epsilon_{SF}(1.4)} - 1 = \frac{4453.8}{(2121 \times 1.4)} - 1 = \underline{0.50}$$

TABLE 8.2.2-II POST CAP ELEMENT PRINCIPAL STRAINS SUMMARY

	TOP		BOTTOM	
CASE	$\in_{MAX}$ (μ in/in)	$\in_{MIN}$ (μ in/in)	$\in_{MAX}$ (μ in/in)	$\in_{MIN}$ (μ in/in)
101	1466	-1181	2163	-1574
102	1523	-1721	2617←	-2147
103	1074	-1880	1459	-1836
104	1529	-1650	2207	-2563←
105	1357	-1161	1445	-1365
106	934	-834	1573	-1077
107	1531←	-1860←	2348	-2147
108	814	-1001	1137	--1504
109	1007	-1141	1584	-1750
110	943	-937	2018	-1324
111	971	-1012	1350	-1310
112	1000	-1235	1173	-1261

Max $\in_{SF}$ = 2592 μ-in/in ($\in_{MIN}$, bottom, case 102)

EL = 20497

$\in_{ULT}$ at Surface = $\in_{US}$ = 1.3(0.003426) [Ref. D683-30037-3, page 8.2.1-12]

= 4454 μ-in/in

$$M.S._{ULT} = \frac{\in_{ULT}}{\in_{SF}(1.4)} - 1 = \frac{4453.8}{(2592 \times 1.4)} - 1 = \underline{0.23}$$

8.2.3 Noodle Bending and Pull Off

Noodle bending and pull off are checked by the methods shown in Ref. D683-30037-3, sections 8.2.1.8.8 and 8.2.1.8.9, and Ref. Memo 28F55-JPH/97-042. All load cases were solved and FEMAP was used to determine maximum and minimum values of internal forces in the post. The margins below are written against the integrated rack loads as well as loads from the individual component accelerations. These values are shown in Tables 8.2.3-I and 8.2.3-II.

It should also be noted that axial shear force check for the posts is not shown. The loads are small and the failure mode is considered OK by inspection.

Maximum limit loads from Tables 8.2.3-I and 8.2.3-II are: (note an extrapolation factor of 1.5 used with F_Y)

	Integrated Loads	Component Loads
M_{YMAX} (model) in-lbs/in	42.6 / -44.2	93.3 / -93.4
F_{YMAX} (model) lbs/in	286.4 / -332.5	450.5 / -501.0
F_{YMAX} (w/ factor) lbs/in	429.6 / -498.8	675.8 / -751.5

Noodle Bending Check

Limit Noodle Moment Allowable = 126 in-lb/in
Ultimate Noodle Moment Allowable = 242 in-lb/in

Integrated Loads	Component Loads
$M.S._{lim} = (126/44.2) - 1 = \underline{1.85}$ (Large)	$M.S._{lim} = (126/93.4) - 1 = \underline{0.35}$
$M.S._{ult} = (242/(44.2 \times 1.4)) - 1 = \underline{2.91}$ (Large)	$M.S._{ult} = (242/(93.4 \times 1.4)) - 1 = \underline{0.85}$

Pull Off Check

Limit Axial Pull Off Allowable = 686 in-lb/in
Ultimate Axial Pull Off Allowable = 1151 in-lb/in

Integrated Loads	Component Loads
$M.S._{lim} = (686/498.8) - 1 = \underline{0.38}$	$M.S._{lim} = (686/751.5) - 1 = \underline{-0.09}$
$M.S._{ult} = (1151/(498.8 \times 1.4)) - 1 = \underline{0.65}$	$M.S._{ult} = (1151/(751.5 \times 1.4)) - 1 = \underline{0.09}$

TABLE 8.2.3-I MAX LOADS FROM COMPONENT ACCELERATIONS

Title : Max/Min Summary of Web Forces, Component Load Factors

Final MAX/MIN Summary Table		Set	ID	Value
Plate X Membrane Force	Minimum	1	21438	-939.006
	Maximum	4	21363	969.154
Plate Y Membrane Force	Minimum	4	21343	-500.953
	Maximum	5	21343	450.543
Plate XY Membrane Force	Minimum	2	21341	-901.158
	Maximum	7	21341	774.85
Plate X Bending Force	Minimum	2	21638	-43.6558
	Maximum	7	21638	41.6958
Plate Y Bending Force	Minimum	3	21486	-93.3939
	Maximum	6	21486	93.2949
Plate XY Bending Force	Minimum	6	21430	-24.2302
	Maximum	3	21430	24.9782
Plate X TransShear Force	Minimum	2	21638	-63.8421
	Maximum	7	21638	61.6003
Plate Y TransShear Force	Minimum	7	21487	-259.356
	Maximum	2	21487	260.655

TABLE 8.2.3-II LOADS FROM INTEGRATED RACK ACCELERATIONS

Final MAX/MIN Summary Table		Set	ID	Value
Plate X Membrane Force	Minimum	3	21385	-619.776
	Maximum	9	21574	759.646
Plate Y Membrane Force	Minimum	11	21416	-332.451
	Maximum	8	21420	286.422
Plate XY Membrane Force	Minimum	8	21418	-595.64
	Maximum	6	21418	649.953
Plate X Bending Force	Minimum	7	21638	-23.292
	Maximum	4	21563	22.0789
Plate Y Bending Force	Minimum	2	21638	-44.2205
	Maximum	8	21499	42.5823
Plate XY Bending Force	Minimum	2	21411	-6.77662
	Maximum	4	21411	7.28554
Plate X TransShear Force	Minimum	7	21563	-34.4407
	Maximum	4	21563	36.8296
Plate Y TransShear Force	Minimum	2	21639	-86.8111
	Maximum	4	21639	79.059

8.2.4 Fastener Analysis

Fastener loads at the payload to rack post interface are derived by examination of the forces of multi-point constraints used to model the fasteners. All loads cases were solved and then searched for their absolute maximum force value. These results for both component and integrated rack loads are shown in Table 8.2.4-I. Load case 104 was identified as the worst case, with node 162440 the most severely loaded fastener. Results are shown below.

TABLE 8.2.4-I FASTENER LOADS SUMMARY (.25 Nom Dia, .257 true)

	Integrated Rack Loads		Component Loads	
Case	Max P_{tot} (lbs)	Node	Max P_{tot} (lbs)	Node
101	1092	21255	2511	163440
102	1140	62446	2460	162446
103	1148	20810	2403	163446
104	1104	62446	>2591<	162440
105	1101	21193	2351	162440
106	1417	62446	2166	163446
107	1260	21193	2224	162446
108	1382	62446	2270	163440
109	1078	20810	n/a	n/a
110	1381	62446	n/a	n/a
111	1049	20810	n/a	n/a
112	1134	21193	n/a	n/a

Ref. D683-30037-3, Pg. 8.14.10

Fbr_{ALL} = (Fbru)(Kd)(Kdt)(Kcsk)(Ksh)(Ked)

Fbru = 80 ksi

dia = 0.25 → Kd = 1.0

d/E ≈ 1, Kdt = 0.88

Nocsk, Kcsk = 1.0

ts/t = 0.02/0.252 = 0.08 → Ksh = 0.95

e/D = 0.80/0.257 = 3.11 → Ked = 1.0

Fbr_{ALL} = (80)(1.0)(0.88)(1.0)(0.95)(1.0) = 66.88 ksi

Pbr_{ALL} = (Fbr_{ALL} x D x t)/Fs = (66.88)(0.257)(0.252)/2 = 2.1657 k

Fastener Shear Allowable = 4.66 k

Pbr_{ALL} Controls

Integrated Loads, M.S. = 2.1657/1.382 - 1 = 0.57

Components Loads, M.S. = 2.1658/2.591 - 1 = - 0.16

8.3 Temperature Case

The effects of thermal loads are typically small and were ignored in the preliminary analysis. To verify the magnitude of the thermal loads for the CIR, a thermal load case was run for a delta temperature of +36°F. A reference temperature of 70°F was assumed. Rack reactions at elevated temperature are shown in Table 8.3-I, and Rack reactions due to each of the twelve inertial load cases are shown in Tables 8.3-II - 8.3-XIII. Maximum/minimum values of the inertial reactions are compared with temperature reactions in Table 8.3-XIV. It is apparent that thermal effects are low enough to be neglected in this preliminary analysis.

TABLE 8.3-I REACTION FORCES, TEMPERATURE

GRID	Fx (lbs)	Fy (lbs)	Fz (lbs)
8019	2.036270E+00	-3.570666E+01	6.821210E-13
8051	-2.960489E+02	-1.916260E+02	4.547474E-13
8073	8.526513E-13	2.273327E+02	0.0
28222	2.940126E+02	4.897335E+01	5.808440E+02
28775	0.0	-4.897335E+01	-5.808440E+02

TABLE 8.3-I I CASE 101, REACTION FORCES

GRID	Fx (lbs)	Fy (lbs)	Fz (lbs)
8019	2.149353E+01	1.884598E+03	-9.566626E+00
8051	-4.734882E+03	-3.052989E+03	-1.838761E+01
8073	-9.821100E+00	-3.901873E+03	-7.370583E+00
28222	-6.288133E+03	-3.885093E+03	-7.591854E+03
28775	0.0	-3.259389E+03	-2.787117E+03

TABLE 8.3-III CASE 102, REACTION FORCES

GRID	Fx (lbs)	Fy (lbs)	Fz (lbs)
8019	2.405685E+01	1.097019E+03	7.531284E+00
8051	-4.760139E+03	-3.107526E+03	1.981280E+01
8073	-9.821100E+00	-4.566605E+03	9.550822E+00
28222	-6.265438E+03	-3.409530E+03	3.122549E+03
28775	0.0	-2.691055E+03	7.268149E+03

TABLE 8.3-IV CASE 103, REACTION FORCES

GRID	Fx (lbs)	Fy (lbs)	Fz (lbs)
8019	-2.179062E+01	-7.049356E+03	-7.531351E+00
8051	4.790936E+03	3.087859E+03	-1.981280E+01
8073	9.821100E+00	-1.114122E+03	-9.550845E+00
28222	6.232375E+03	-3.424627E+03	-3.187868E+03
28775	0.0	-3.689072E+03	-7.202830E+03

TABLE 8.3-V CASE 104, REACTION FORCES

GRID	Fx (lbs)	Fy (lbs)	Fz (lbs)
8019	-2.159018E+01	-2.810755E+02	-7.531294E+00
8051	4.468167E+03	2.914652E+03	-1.981279E+01
8073	1.055630E+01	3.950727E+03	-9.550828E+00
28222	6.409171E+03	4.164714E+03	-2.968282E+03
28775	0.0	1.903251E+03	-7.422416E+03

TABLE 8.3-VI CASE 105, REACTION FORCES

GRID	Fx (lbs)	Fy (lbs)	Fz (lbs)
8019	1.676063E+01	7.020993E+03	-9.566549E+00
8051	-4.473707E+03	-2.840449E+03	-1.838761E+01
8073	-1.055630E+01	2.394732E+03	-7.370555E+00
28222	-6.398802E+03	2.193879E+03	-7.680801E+03
28775	0.0	3.908542E+03	-2.698169E+03

TABLE 8.3-VII CASE 106, REACTION FORCES

GRID	Fx (lbs)	Fy (lbs)	Fz (lbs)
8019	2.137634E+01	2.902174E+03	8.170991E+00
8051	-3.989457E+03	-2.576870E+03	1.522133E+01
8073	-5.322620E+00	-2.271156E+03	5.874388E+00
28222	-6.918932E+03	-5.115243E+03	4.395771E+03
28775	0.0	-5.153650E+03	6.284333E+03

TABLE 8.3-VIII CASE 107, REACTION FORCES

GRID	Fx (lbs)	Fy (lbs)	Fz (lbs)
8019	2.395492E+01	-1.125401E+03	-6.135727E+00
8051	-4.016930E+03	-2.632841E+03	-1.664659E+01
8073	-5.322620E+00	-5.939609E+03	-8.054684E+00
28222	-6.894036E+03	-1.399048E+03	-6.589751E+03
28775	0.0	-1.580797E+03	-4.102081E+03

TABLE 8.3-IX CASE 108, REACTION FORCES

GRID	Fx (lbs)	Fy (lbs)	Fz (lbs)
8019	-1.890967E+01	-2.086231E+03	-8.171000E+00
8051	3.697485E+03	2.383997E+03	-1.522133E+01
8073	6.057822E+00	1.655278E+03	-5.874393E+00
28222	7.062664E+03	5.870427E+03	-4.241504E+03
28775	0.0	4.365847E+03	-6.438600E+03

TABLE 8.3-X CASE 109, REACTION FORCES

GRID	Fx (lbs)	Fy (lbs)	Fz (lbs)
8019	-1.932395E+01	-6.233413E+03	-7.531361E+00
8051	4.498964E+03	2.894985E+03	-1.981279E+01
8073	1.055630E+01	-1.730000E+03	-9.550851E+00
28222	6.376107E+03	-2.669442E+03	-3.033601E+03
28775	0.0	-4.476875E+03	-7.357097E+03

TABLE 8.3-XI CASE 110, REACTION FORCES

GRID	Fx (lbs)	Fy (lbs)	Fz (lbs)
8019	2.148590E+01	3.504596E+03	6.135688E+00
8051	-4.733773E+03	-3.052272E+03	1.664656E+01
8073	-9.821100E+00	-2.400012E+03	8.054655E+00
28222	-6.289233E+03	-5.505409E+03	3.258109E+03
28775	0.0	-4.761648E+03	7.433723E+03

TABLE 8.3-XII CASE 111, REACTION FORCES

GRID	Fx (lbs)	Fy (lbs)	Fz (lbs)
8019	-1.921439E+01	-5.630991E+03	-9.566664E+00
8051	3.754647E+03	2.419583E+03	-1.838757E+01
8073	6.057822E+00	-1.858857E+03	-7.370583E+00
28222	7.005806E+03	-3.059608E+03	-4.171264E+03
28775	0.0	-4.084874E+03	-6.207707E+03

TABLE 8.3-XIII CASE 112, REACTION FORCES

GRID	Fx (lbs)	Fy (lbs)	Fz (lbs)
8019	-1.665106E+01	-6.418571E+03	7.531246E+00
8051	3.729391E+03	2.365047E+03	1.981283E+01
8073	6.057822E+00	-2.523588E+03	9.550822E+00
28222	7.028500E+03	-2.584045E+03	6.543139E+03
28775	0.0	-3.516540E+03	3.847560E+03

TABLE 8.3-XIV MIN/MAX REACTION FORCES VS. THERMAL REACTION FORCES

		Load Case	GRID	Inertial Reaction (lbs)	Thermal Reaction (lbs)
Fx	Minimum	103	8019	-21.7906	
	Maximum	102	8019	24.0569	2.04
Fy	Minimum	103	8019	-7049.36	
	Maximum	105	8019	7020.99	-35.7
Fz	Minimum	111	8019	-9.56666	
	Maximum	106	8019	8.17099	0
Fx	Minimum	102	8051	-4670.14	
	Maximum	103	8051	4790.94	-296.0
Fy	Minimum	102	8051	-3107.53	
	Maximum	103	8051	3087.86	-191.6
Fz	Minimum	103	8051	-19.8128	
	Maximum	112	8051	19.8128	0
Fx	Minimum	105	8073	-10.5563	
	Maximum	104	8073	10.5563	0
Fy	Minimum	107	8073	-5939.61	
	Maximum	104	8073	3950.73	227.3
Fz	Minimum	109	8073	-9.55085	
	Maximum	102	8073	9.55082	0
Fx	Minimum	106	28222	-6918.93	
	Maximum	108	28222	7062.66	294.0
Fy	Minimum	110	28222	-5505.41	
	Maximum	108	28222	5870.43	49.0
Fz	Minimum	105	28222	-7680.8	
	Maximum	112	28222	6543.14	580.8
Fx	Minimum	101	28775	0	
	Maximum	101	28775	0	0
Fy	Minimum	106	28775	-5153.65	
	Maximum	108	28775	4365.85	-99.0
Fz	Minimum	104	28775	-7422.42	
	Maximum	110	28775	7433.72	-580.8

TABLE 8.3-XV INERTIAL LOAD CASES REF

CASE	Nx (g's)	Ny (g's)	Nz (g's)	αx (rad/sec$_2$)	αy (rad/sec$_2$)	αz (rad/sec$_2$)
101	7.00	8.00	6.80	70.8	18.2	34.8
102	7.00	8.00	-6.80	-70.8	18.2	34.8
103	-7.00	8.00	6.80	70.8	-18.2	-34.8
104	-7.00	-8.00	6.80	70.8	-18.2	34.8
105	7.00	-8.00	6.80	70.8	18.2	-34.8
106	7.00	8.00	-6.80	70.8	-18.2	34.8
107	7.00	8.00	6.80	-70.8	-18.2	34.8
108	-7.00	-8.00	6.80	-70.8	18.2	34.8
109	-7.00	8.00	6.80	70.8	-18.2	34.8
110	7.00	8.00	-6.80	70.8	18.2	34.8
111	-7.00	8.00	6.80	70.8	18.2	34.8
112	-7.00	8.00	-6.80	-70.8	18.2	34.8